Unlocking the secrets of kangaroo locomotor energetics: Postural adaptations underpin increased tendon stress in hopping kangaroos.

Lauren H. Thornton[1], Taylor J.M. Dick[2], John R. Hutchinson[3], Glen A. Lichtwark[4], Craig P. McGowan[5], Jonas Rubenson[6], Alexis Wiktorowicz-Conroy[3], Christofer J. Clemente[1,2]

[1]School of Science, Technology, and Engineering, University of the Sunshine Coast, Sippy Downs, Queensland, Australia

[2]School of Biomedical Sciences, University of Queensland, St Lucia, Queensland, Australia

[3]Structure and Motion Lab, Department of Comparative Biomedical Sciences, The Royal Veterinary College, Hawkshead Lane, Hatfield, Hertfordshire, United Kingdom

[4]School of Exercise and Nutrition Science, Queensland University of Technology, Brisbane, Queensland, Australia

[5]Department of Integrative Anatomical Sciences, Keck School of Medicine University of Southern California, Los Angeles, California, USA

[6]Biomechanics Laboratory, Department of Kinesiology, The Pennsylvania State University, University Park, PA 16802, USA

Abstract

Hopping kangaroos exhibit remarkably little change in their rate of metabolic energy expenditure with locomotor speed compared to other running animals. This phenomenon may be related to greater elastic energy savings due to increasing tendon stress; however, the mechanisms which enable the rise in stress remain poorly understood. In this study, we created a three-dimensional (3D) kangaroo musculoskeletal model, integrating 3D motion capture and force plate data, to analyse the kinematics and kinetics of hopping red and grey kangaroos. Using our model, we evaluated how body mass and speed influence (i) hindlimb posture, (ii) effective mechanical advantage (EMA), and (iii) the associated tendon stress in the ankle extensors and (iv) ankle work during hopping. We found that increasing ankle dorsiflexion and metatarsophalangeal plantarflexion likely played an important role in decreasing ankle EMA by altering both the muscle and external moment arms, which subsequently increased energy absorption and peak tendon stress at the ankle. Surprisingly, kangaroo hindlimb posture appeared to contribute to increased tendon stress, thereby elucidating a potential mechanism behind the increase in stress with speed. These posture-mediated increases in elastic energy savings could be a key factor enabling kangaroos to achieve energetic benefits at faster hopping speeds, but may limit the performance of large kangaroos due to the risk of tendon rupture.

Introduction

Kangaroos and other macropods are unique in both their morphology and their locomotor style. At slow speeds they use a pentapedal gait, where the forelimbs, the hindlimbs, and the tail all contact the ground, while at faster movement speeds they use their distinctive hopping gait (Dawson and Taylor 1973, O'Connor et al. 2014). Their uniqueness extends into their energetics of locomotion. As far back as the 19th century, researchers noticed that the metabolic cost of running in quadrupeds and bipeds, like dogs, horses and humans, increased linearly with speed (Zuntz 1897, Taylor et al. 1970, Heglund et al. 1982, Taylor et al. 1982). To explain why metabolic rate increased at faster running speeds among quadrupeds and bipeds, Kram and Taylor (1990) refined the 'cost of generating force' hypothesis (Taylor et al. 1980). They reasoned that the decrease in contact time with increased speed, reflects an increase in the rate of generating muscle force, and the rate of cross-bridge cycling (Kram and Taylor 1990). This was supported for a diverse range of running animals, suggesting that metabolic rate was inversely proportional to contact time (Kram and Taylor 1990). Yet hopping macropods appear to defy this trend. On treadmills, both red kangaroos (~20 kg) and tammar wallabies (~5 kg) showed little to no increase in the rate of oxygen consumption with increased hopping speed (Dawson and Taylor 1973, Baudinette et al. 1992, Kram and Dawson 1998). The underlying mechanisms explaining how macropods are able to uncouple hopping speed and energy cost is not completely understood (Thornton et al. 2022).

The ability to uncouple speed and energy expenditure in macropods is related to the behaviour of their ankle extensor muscle-tendon units, which store and return elastic strain energy (Morgan et al. 1978, Biewener et al. 2004b, McGowan et al. 2005). In tammar wallabies, ankle tendon stress increased with hopping speed, leading to a greater rise in elastic strain energy return than muscle work, which increases the proportion of work done by tendon recoil while muscle work remains near constant (Baudinette and Biewener 1998, Biewener et al. 1998). Size-related differences in ankle extensor tendon morphology (Bennett and Taylor 1995, McGowan et al. 2008), and the resultant low strain energy return, may explain why small (<3 kg) hopping macropods and rodents appear not to be afforded the energetic benefits observed in larger macropods (Thompson et al. 1980, Biewener et al. 1981, Biewener et al. 1998) (but see Christensen et al. (2022)). However tendon morphology alone is insufficient to explain why large macropods can increase speed without cost, while large quadrupeds with similar tendon morphology cannot (Dawson and Webster 2010). The most obvious difference between macropods and other mammals is their hopping gait, but previously proposed mechanisms to explain how hopping could reduce the metabolic cost of generating muscle force, such as near-constant stride frequency (Heglund and Taylor 1988, Dawson

and Webster 2010) or respiratory-stride coupling (Baudinette et al. 1987), do not distinguish between small and large macropods, nor galloping quadrupeds (McGowan and Collins 2018).

Postural changes are another mechanism which could contribute to reduced energetic costs by altering the leverage of limb muscles. The effective mechanical advantage (EMA) is the ratio of the internal muscle-tendon moment arm (the perpendicular distance between the muscle's force-generating line-of-action and the joint centre) and the ground reaction force (GRF) moment arm (the perpendicular distance between the vector of the GRF to the joint centre). Smaller EMA requires greater muscle force to produce a given force on the ground, thereby demanding a greater volume of active muscle, and presumably higher metabolic rates. In humans, an increase in limb flexion and decrease in limb EMA recruits a greater volume of muscle and increases the metabolic cost of running compared to walking (Biewener et al. 2004a, Kipp et al. 2018, Allen et al. 2022). Elephants—one of the largest and noticeably most upright animals, do not have discrete gait transitions, but rather continuously and substantially decrease EMA in limb joints when moving faster, which has also been linked to the increase in metabolic cost of locomotion with speed (Ren et al. 2010, Langman et al. 2012). EMA has also been observed to change with size in terrestrial mammals. Smaller animals tend to move in crouched postures with limbs becoming progressively more extended as body mass increases (Biewener 1989). Yet, rather than metabolic cost, this postural transition appeared to be driven by the need to reduce the size-related increases in tissue stress (Dick and Clemente 2017, Clemente and Dick 2023). As a consequence of transitioning to more upright limb postures, musculoskeletal stresses in terrestrial mammals are independent of body mass (Biewener 1989, 2005).

Macropods, in contrast, maintain a crouched posture during hopping. Kram and Dawson (1998) explored whether kangaroos transitioned to a more extended limb posture with increasing speed as a potential mechanism for their constant metabolic rate, but did not detect a change in EMA at the ankle across speeds from 4.3 to 9.7 m s^{-1}. Further, ankle posture and EMA appears to vary weakly (McGowan et al. 2008) or not at all with body mass in macropods (Bennett and Taylor 1995, Snelling et al. 2017). As a consequence, stress would be expected to increase with both hopping speed and body mass. High tendon stresses are required for high strain energy return (strain energy $\propto$ $stress^2$) (Biewener and Baudinette 1995). Given that tendon recoil plays a pivotal role in hopping gaits, it is perhaps unsurprising that tendon stress approaches the safe limit in larger kangaroos. The ankle extensor tendons in a moderately sized male red kangaroo (46.1 kg) operate with safety factors near two even at slow hopping speeds (3.9 m s^{-1}) (Kram and Dawson 1998). Tendon stresses are also unusually high in smaller kangaroos. Juvenile and adult western grey kangaroos, ranging in mass from 5.8 to 70.5 kg, all hop with gastrocnemius and plantaris tendon safety factors less than two

(Snelling et al. 2017). High tendon stress may not only be a natural consequence of their crouched posture and tendon morphology , but also adaptively selected. Considering this, kangaroos may adjust their posture to increase tendon stress and its associated elastic energy return. If so, there would likely be systematic variation in kangaroo posture with speed and mass—which is yet to be fully explored.

In this study, we investigate the hindlimb kinematics and kinetics in kangaroos hopping at their preferred speed. Specifically, we explore the relationship between changes in posture, EMA, joint work, and tendon stress across a range of hopping speeds and body masses. To do this, we built a musculoskeletal model of a kangaroo based on empirical imaging and dissection data (Fig. 1a). We used the musculoskeletal model to calculate ankle EMA throughout the stride by capturing changes in both muscle moment arm and the GRF moment arm, allowing us to explore their individual contributions. We hypothesised that (i) the distal hindlimb, and the ankle joint in particular, would be more flexed when hopping at faster speeds and larger sizes, and (ii) the change in posture and moment arms would contribute to the increase in tendon stress with speed, and may thereby contribute to energetic savings by increasing the amount of positive and negative work done by the ankle.

Results

Ground reaction forces

The stance begins with a breaking phase (negative horizontal component), followed by a propulsive phase (positive horizontal component). At the transition from negative to positive, the GRF was vertical, and this occurred at 42.9±26.9% of stance. The peak in vertical GRF, however, occurred at 46.4±5.3% of stance (Fig. 2a,b).

Larger kangaroos and faster speeds were associated with greater magnitudes of peak GRFs (Fig. 2a,b; Suppl. Table 2). When peak vertical GRF was normalised to body weight, peak forces ranged from 1.4 multiples of body weight (BW) to 3.7 BW per leg (mean: 2.41±0.396 BW) and increased with speed (Suppl. Fig. 2a). Smaller kangaroos may experience disproportionately greater GRFs at faster speeds (Suppl. Fig. 2b, Suppl. Table 2).

Kinematics and posture

Kangaroo hindlimb kinematics varied with both body mass and speed. Higher masses and faster speeds were associated with more crouched hindlimb postures (Fig. 3a,c). Size-related changes in

141 posture occurred throughout stance and were distributed as small changes among all hindlimb joints
142 rather than a large shift in any one joint (Fig. 3d,f; Suppl. Table 3). The hip, knee and ankle tended
143 toward more flexion, and the metatarsophalangeal (MTP) toward greater plantarflexion in larger
144 kangaroos.

145 In addition to, and independent of, the change in posture with mass, there were substantial postural
146 changes due to speed (Suppl. Table 3). Unlike with mass, speed-related changes occurred
147 predominantly during the braking phase, and the change was concentrated in the ankle and MTP
148 joints, with little to no change in the proximal joints (Fig. 3c,e,g; Suppl. Table 3). There was a
149 significant decrease in ankle plantarflexion at initial ground contact and increase in dorsiflexion at
150 midstance at faster speeds (Fig. 3g; Suppl. Table 3). Maximum ankle dorsiflexion occurred at
151 44.8±4.5% of stance, and tended to occur 3.9±0.7% earlier in stance with each 1 m s^{-1} increase in
152 speed ($P<0.001$). MTP range of motion increased with speed due to an increase in MTP
153 plantarflexion prior to midstance rather than a change in dorsiflexion (Fig. 3g).

154 Effective Mechanical Advantage

155 Effective mechanical advantage (EMA) decreased as the limb became more crouched. The change in
156 EMA with mass and speed was substantial, particularly in the braking period (Fig. 2c,d). We
157 evaluated the change in EMA at midstance, as it was approximately the point in the stride where
158 GRF (and therefore tendon stress) was highest. EMA at midstance decreased with body mass,
159 although we did not detect an effect of speed (Fig. 2c,d; Suppl. Table 5). However, examining
160 whether the decrease in EMA was caused by a decrease in the muscle moment arm, *r*, or an increase
161 in the external moment arm, *R*, revealed a more nuanced picture.

162 Speed, rather than body mass, was associated with a decrease in *r* at midstance (Suppl. Fig. 3a,b;
163 Suppl. Table 5). A kangaroo travelling 1 m s^{-1} faster would decrease *r* by approximately 4.2%. The
164 muscle moment arm reduced with speed for the full range of speeds we measured (1.99 – 4.48 m s^{-}
165 ^{1}), with the maximum *r* occurring when the ankle was at 114.4±0.8°. Maximum ankle dorsiflexion
166 ranged from 114.5° in the slowest trials, to 75.8° in faster trials (Suppl. Fig. 3g). The timing of the
167 local minimum *r* at midstance coincided with the timing of peak ankle dorsiflexion.

168 We observed an increase in *R* with body mass, but not speed, at midstance (Suppl. Fig. 3c,d; Suppl.
169 Table 5). We expected *R* to vary with both mass and speed because the increase in MTP
170 plantarflexion prior to midstance reduced the distance between the ankle joint and the ground,
171 which would increase *R* since the centre of pressure (CoP) at midstance remained in the same
172 position (Fig. 6, Suppl. Table 2). Increasing body mass by 4.6 kg or speed by 1 m s^{-1} resulted in a ~20%
173 reduction in ankle height (Suppl. Fig. 3e,f). Although, posture alone may not account for the change

in *R*, as the metatarsal segment also increased in length with body mass (1 kg BM corresponded to ~1% longer segment, $P<0.001$, $R^2=0.449$).

Joint moments

The change in the muscle moment arm, *r*, with speed has further implications for Achilles tendon stress, because force in the tendon is determined by the ratio of the ankle moment to *r* (Fig. 6). As such, the decrease in *r* with speed would tend to increase tendon force (and thereby tendon stress), as would an increase in ankle moment. We found that speed, rather than mass, was associated with an increase in the maximum ankle moment (Suppl. Fig. 4; Suppl. Table 4, see supplementary material for details on other hindlimb joint moments).

Tendon stress

Peak tendon stress increased as minimum EMA decreased (Fig. 7a). Small decreases in EMA correspond to a nontrivial increase in tendon stress, for instance, reducing EMA from 0.242 (mean minimum EMA of the slow group) to 0.206 (mean minimum EMA of the fast group) was associated with an ~18% increase in tendon stress. Tendon stress increased with body mass and speed (Suppl. Table 5). Maximum stress in the ankle extensor tendons occurred at 46.8±4.9% of stance, aligning with the timing of peak vertical GRF and maximum ankle moment. Body mass did not have a significant effect on the timing of peak stress, but peak stress occurred 3.2±0.8% earlier in stance with each 1 m s^{-1} increase in speed ($P<0.001$), reflecting the timing of the peak in ankle dorsiflexion.

Joint work and power

An analysis of joint-level energetics showed the majority of work and power in the hindlimb was performed by the ankle joint (Fig. 4; Suppl. Table 8). The ankle performed negative work in the braking period, as kinetic and gravitational potential energy was transferred to elastic potential energy by loading the ankle extensor tendons. An increase in negative ankle work was associated with the increase in tendon stress in the ankle extensors ($B=0.750$, $SE=0.074$, $P<0.001$, $R^2=0.511$). Simple linear regression indicated that the increase in negative work was associated with speed but not body mass (Fig. 5a; Suppl. Fig. 5e,f; Suppl. Table 6).

Elastic potential energy was returned to do positive work in the propulsive period as the ankle started extending prior to midstance. Positive ankle work increased with both mass and speed (Fig. 5a; Suppl. Fig. 5e,f; Suppl. Table 6), but since it increased at the same rate as negative work, critically, there was no change in net ankle work with speed (Fig. 5b; Suppl. Fig. 6e,f; Suppl. Table 6).

Discussion

How does posture contribute to kangaroo energetics?

The cost of generating force hypothesis (Taylor et al. 1980) implies that as animals increase locomotor speed and decrease ground contact time, metabolic rate should increase (Kram and Taylor 1990). Macropods defy this trend (Dawson and Taylor 1973, Baudinette et al. 1992, Kram and Dawson 1998). It is likely that the use of their ankle extensor tendons set them apart from other mammals, yet the underlying mechanisms for this were unclear (Bennett and Taylor 1995, Bennett 2000, Thornton et al. 2022). We hypothesised (i) the distal hindlimb would be more flexed when hopping at faster speeds and larger masses, mainly due to the ankle, and (ii) the change in posture and EMA would contribute to the increase in tendon stress.

Tendon stress depends on the muscle moment arm, ankle moment, external moment arm, and ground reaction force (GRF), assuming tendon properties remain unchanged (Fig. 6). We detected an increase in peak ankle moment with speed independent of increases in body mass, despite the change in the external moment arm, *R*, with mass, likely due to a dominant effect of the GRF (ankle moment = GRF · *R*). Peak GRFs varied with speed as well as mass. Both the increase in ankle moment and a decrease in *r* with speed tend to increase tendon stress (stress = tendon force / cross-sectional area; tendon force = ankle moment / *r*). Although the increase in peak GRF with speed explains much of the increase in tendon stress, the significant relationship between tendon stress and ankle EMA suggests that the increase in stress is not solely due to the greater GRFs, but that stress may also be modulated by changes in posture throughout the stride (Fig. 7a).

Previously, macropods were reported to have consistent ankle EMA due to the muscle moment arm, *r*, and the external moment arm, *R*, scaling similarly with body mass (Fig. 7b) (Bennett and Taylor 1995). Our results, however, suggest posture is not as consistent or static as previously reported if speed is taken into account; we found larger and faster kangaroos were more crouched, leading to lower ankle EMA (Fig. 2c,d). We were able to explore the individual contributions to ankle EMA using our musculoskeletal model, to demonstrate that changes in the ankle and metatarsophalangeal (MTP) range of motion resulted in changes in *r* with speed, and *R* with mass, respectively. These effects were additive; combined, there was a marked decrease in ankle EMA, particularly during the early stance when the ankle extensor tendons are loaded (Fig. 2c,d). As such, the change in ankle EMA appears to be a mechanism that contributes to the increase in tendon stress (Fig. 7a) and ankle work (Fig. 5a).

Kangaroos appear to use changes in posture and EMA to absorb and return energy during stance. A comparison among all the hindlimb joints suggests the ankle was primarily responsible for both the storage and release of work during the stride (Fig. 4). Positive work increased with mass and speed, consistent with other studies in other species (Cavagna and Kaneko 1977). However, critically, the amount of negative work absorbed during the stride also increased with speed, and net ankle work did not change with speed, indicating the increase in negative work absorbed matched the increase in positive work that is required to move forward (Fig. 5b). Indeed, we observed all trials had a similar positive net ankle work (mean: 0.67 ± 0.54 J kg^{-1}). The consistent net work observed among all speeds suggests the ankle extensors are performing similar amounts of ankle work independent of speed. Previous studies using sonomicrometry have shown that the muscles of tammar wallabies do not shorten considerably during hops, but rather act near-isometrically as a strut (Biewener et al. 1998). Further, these small changes in muscle fibre length did not vary with hopping speed, despite large increases in muscle tendon forces (Biewener et al. 1998). Isometric muscle contractions are efficient (Smith et al. 2005). The cost of generating force hypothesis suggests that faster movement speeds require greater rates of muscle force development, and in turn greater cross bridge cycling rates, driving up metabolic costs (Taylor et al. 1980, Kram and Taylor 1990). The ability for the ankle extensor muscle fibres to remain isometric and produce similar amounts of work at all speeds may help explain why hopping macropods do not follow the energetic trends observed in quadrupedal species. Their ability to do this requires the amount of negative work to increase with speed. Modifying the ankle EMA as speed increases allows an increase in tendon stress (Fig. 7a) enabling the storage of more energy during the first half of stance. Since the muscle remains near isometric, no additional work is performed by the muscle, but the overall positive work increases, likely owing to the greater return of elastic strain energy, and enabling faster hopping speeds (Fig. 6). Thus, changes in EMA provide a likely mechanism to explain the uncoupling of metabolic energy expenditure with locomotor speed observed in large hopping macropods (Dawson and Taylor 1973, Baudinette et al. 1992, Kram and Dawson 1998).

Why are macropods unique?

No other mammals are known to achieve the same energetic feat as macropods, despite similar tendons or stride parameters (Thornton et al. 2022), but macropods are unique in other ways. Kangaroos operate at much lower EMA values than other mammalian species (Fig. 7b). Mammals >18 kg tend to operate with EMA values 0.5 to 1.2. The only mammals with comparable EMA values to kangaroos are rodents <1 kg (Fig. 7b) (Biewener 1990), such as kangaroo rats which have relatively thicker tendons that may be less suited for recovering elastic strain energy (Biewener and Blickhan 1988) (but see: Christensen et al. (2022)). Fig. 7a shows the non-linear relationship between

tendon stress and EMA in kangaroos, quadrupeds and humans. The range of EMA estimates for other mammals suggest they operate in the region of this curve where large changes in EMA would only produce small changes in stress. This implies EMA modulation in other species is not as effective a mechanism to increase tendon stress with increased running speed as that observed in kangaroos.

Were macropods performance or size limited?

The morphology and hopping gait that make kangaroos supremely adapted for efficient locomotion likely also have several performance limitations. One possible consequence is a predicted reduction in manoeuvrability (Biewener 2005). The high compliance of the tendon would limit the ability to rapidly accelerate, owing to the lag between muscle force production and the transmission of this force to the environment. A second important limitation is the requirement for kangaroos to operate at high tendon stresses. Previous research has suggested that kangaroos locomote at dangerously low safety factors for tendon stress, predicted to be between 1-2 for large kangaroos (Kram and Dawson 1998, McGowan et al. 2008, Snelling et al. 2017, Thornton et al. 2022). Our new insights into the mass and speed modulated changes in EMA suggest that these safety factors may be even lower, likely limiting the maximum body mass that hopping kangaroos can achieve. This suggests that previous projections of tendon stress may have overestimated the body mass at which tendons reach their safety limit ('safety factor' of 1). Snelling et al. (2017) estimated the maximum body mass to remain above this limit was approximately 160 kg, but even if we consider this is a conservative prediction, it is far lower than the projected mass of extinct macropodids (up to 240 kg (Helgen et al. 2006, Janis et al. 2023)). Thus we expect there must be a body mass where postural changes shift from contributing to stress to mitigating it (Dick and Clemente 2017).

This study highlights how EMA may be more dynamic than previously assumed, and how musculoskeletal modelling and simulation approaches can provide insights into direct links between form and function which are often challenging to determine from experiments alone.

Methods

Animals and data collection

Hopping data for red and eastern grey kangaroos was collected at Brisbane's Alma Park Zoo in Queensland, Australia, in accordance with approval by the Ethics and Welfare Committee of the Royal Veterinary College; approval number URN 2010 1051. The dataset includes 16 male and female kangaroos ranging in body mass from 13.7 to 26.6 kg (20.9 ± 3.4 kg). Two juvenile red

302 (*Macropus rufus*) and 11 grey kangaroos (*Macropus giganteus*) were identified, while the remaining
303 three could not be differentiated as either species. Body mass was determined in several ways,
304 primarily by measurements of the kangaroos standing stationary on the force plate. If the individual
305 did not stop on the force plate, and forward velocity was constant, then body mass was determined
306 by dividing the total impulse across a constant velocity hop cycle (foot strike to foot strike) by the
307 total hop cycle time and further dividing by gravitational acceleration. Finally, if neither of these
308 approaches were sufficient, we interpolated from the relationship between leg marker distances (as
309 proxy for segment lengths) and body mass. These methods produce estimates of body masses close
310 to stationary measurements, where both were available.

311 Experimental protocol

312 Kangaroos hopped at their preferred speed down a runway (~10x1.5 m) that was constructed in
313 their enclosure using hessian cloths and stakes (Suppl. Video 1). The runway was open at both ends
314 with two force plates (Kistler custom plate (60x60 cm) and AMTI Accugait plate (50x50 cm)) set
315 sequentially in the centre and buried flush with the surface. The force plates recorded ground
316 reaction forces (GRF) in the vertical, horizontal and lateral directions.

317 A 6-camera 3D motion capture system (Vicon T160 cameras), recorded by Nexus software (Vicon,
318 Oxford, UK) at 200 Hz, was used to record kinematic data. Reflective markers were placed on the
319 animals over the estimated hip, knee, ankle, metatarsophalangeal (MTP) joints; the distal end of
320 phalanx IV; the anterior tip of the ilium; and the base of the tail (Fig. 1a). Force plate data was
321 synchronously recorded at 1000 Hz via an analogue to digital board integrated with the Vicon
322 system.

323 Data analysis

324 We calculated the stride length from the distance between the ankle or MTP marker coordinates at
325 equivalent time points in the stride. The stance phase was defined as the period when the vertical
326 GRF was greater than 2% of the peak GRF. We determined ground contact duration and total stride
327 duration from the frame rate (200 Hz) and the number of frames from contact to take-off (contact
328 duration) and contact to contact (stride duration), respectively, and calculated the stride frequency.
329 Stride parameter results are detailed in the supplementary material.

330 In most trials, the stride before and after striking the force plate was visible, providing a total of 173
331 strides. If two strides were present in a trial, we took the average of the two strides for that trial.
332 Trials were excluded if only one foot landed on the force plate or if the feet did not land near-
333 simultaneously, to give a total of 100 trials. We did not include trials where the kangaroo started
334 from or stopped on the force plate. We assumed GRF was equally shared between each leg and

divided the vertical, horizontal and lateral forces in half, and calculated all results for one leg. We normalised GRF by body weight. We assumed the force was applied along phalanx IV and that there was no medial or lateral movement of the centre of pressure (CoP) (Fig. 1b). The anterior or posterior movement of the CoP was recorded by the force plate within the motion capture coordinate system.

We calculated the hopping velocity and acceleration of the kangaroo in each trial from the position of the pelvis marker, as this marker was close to the centre of mass and there should have been minimal skin movement artefact. Position data were smoothed using the 'smooth.spline' function in R (version 3.6.3). The average locomotor speed of the trial was taken as the mean horizontal component of the velocity during the aerial phase before and after the stance phase.

Building a kangaroo musculoskeletal model

We created a musculoskeletal model based on the morphology of a kangaroo for use in OpenSim (v3.3; Seth et al. (2018)) (Fig. 1a). The skeletal geometry was determined from a computed tomography (CT) scan of a mature western grey kangaroo (MorphoSource.org, Duke University, NC, USA). Western grey kangaroos are morphologically similar to eastern grey and red kangaroos (Thornton et al. 2022).

We extracted the skeletal components from the CT scan using Dragonfly (Version 2020.2, Object Research Systems (ORS) Inc., Montreal, Canada) and partitioned the hindlimb into five segments (pelvis, femur, tibia, metatarsals and calcaneus, and phalanges). The segments were imported into Blender (version 3.0.0, https://www.blender.org/; Amsterdam, Netherlands) to clean and smooth the bones, align the vertebrae, and export the segments as meshes. We imported the meshes into Rhinoceros (version 6.0, Robert McNeel & Associates, Seattle, WA, USA) to construct the framework of the movement system.

All joints between segments were modelled as hinge joints which constrain motion to a single plane and one degree of freedom (DOF), except the hips which were modelled as ball-and-socket joints with three DOF. The joints were restricted to rotational (no translational) movement. The joints were marked with an origin (joint centre) and coordinate system determined by the movement of the segment (x is abduction/adduction, y is pronation/supination, z is extension/flexion). The limb bones and joints from one leg were mirrored about the sagittal plane to ensure bilateral symmetry.

The segment masses for a base model were determined from measurements of eastern grey and red kangaroos provided in Hopwood (1976). Cylinders set to the length and mass of each segment were used to approximate the segment centre of mass and moments of inertia.

We scaled the model to the size and mass of each kangaroo using the OpenSim scale tool. A static posture was defined based on the 3D positions of the markers at midstance. Each segment was scaled separately, allowing for different scaling factors across segments. The markers with less movement of the skin over the joint (e.g. the MTP marker) were more highly weighted than the markers with substantial skin movement (e.g. the hip and knee markers) in the scaling tool.

Joint kinematics and mechanics

We used inverse kinematics to determine time-varying joint angles during hopping. Inverse kinematics is an optimisation routine which simulates movement by aligning the model markers with the markers in the kinematic data for each time step (Suppl. Video 2). We adjusted the weighting on the markers based on the confidence and consistency in the marker position relative to the skeleton. The model movement from inverse kinematics was combined with GRFs in an inverse dynamics analysis to calculate net joint moments for the hip, knee, ankle and MTP joints throughout stance phase. Joint moments were normalised to body weight and leg length.

We calculated instantaneous joint powers for each of the hindlimb joints over the stance phase of hopping as the product of joint moment (not normalised) and joint angular velocity. To determine work, we integrated joint powers with respect to time over discrete periods of positive and negative work, consistent with Dick et al. (2019). For the stance duration of each hop, all periods of positive work were summed and all periods of negative work were summed to determine the positive work, negative work, and net work done at each of the hindlimb joints for a hop cycle. Joint work was normalised to body mass.

Posture and EMA

We evaluated overall hindlimb posture to determine how crouched or upright the hindlimbs were during the stance phase of hopping. The total hindlimb length was determined as the sum of all segment lengths between the joint centres, from the toe to ilium (Fig. 1a). The crouch factor (CF) was calculated as the distance between the toe and the ilium marker divided by the total hindlimb length. Larger CF values indicated extended limbs whereas smaller CF values indicated more crouched postures.

We calculated the effective mechanical advantage (EMA) at the ankle as the muscle moment arm of the combined gastrocnemius and plantaris tendon, r, divided by the external moment arm, R (perpendicular distance between the GRF vector and the ankle joint) (Fig. 1b). We dissected (with approval from University of the Sunshine Coast Ethics Committee, ANE2284) a road-killed 27.6 kg male eastern grey kangaroo and used this, combined with published anatomy on the origin and insertion sites, to determine the ankle extensor muscle-tendon unit paths on the skeleton in

OpenSim (Bauschulte 1972, Hopwood and Butterfield 1976, Hopwood and Butterfield 1990). The value *r* to the gastrocnemius and plantaris tendons for all possible ankle angles were determined from OpenSim and scaled to the size of each kangaroo, while *R* was calculated as the perpendicular distance between the ankle marker and the GRF vector at the CoP.

Tendon stress

Ankle extensor tendon forces were estimated as the time-varying ankle moment divided by the time varying Achilles tendon moment arm. The sum of the gastrocnemius and plantaris tendon cross-sectional areas were scaled to kangaroo body mass for each kangaroo by interpolating literature values (Snelling et al. 2017). Forces were divided by tendon cross-sectional area to calculate tendon stress. We excluded the third ankle extensor tendon (flexor digitorum longus), which stores ~10% of strain energy of the ankle extensors in tammar wallabies (Biewener and Baudinette 1995).

Statistics

We used multiple linear regression (lm function in R, v. 3.6.3, Vienna, Austria) to determine the effects of body mass and speed on the stride parameters, ground reaction forces, joint angles and CF, joint moments, joint work and power, and tendon stress. We considered the interaction of body mass and speed first, and removed the interaction term from the linear model if the interaction was not significant. Effects were considered significant at the $p<0.05$ level. Species was not used as a factor in the analysis as there was no systematic difference in outcome measures between kangaroo species.

Acknowledgements

We thank the Brisbane Alma Park Zoo for hosting and facilitating this work; particularly Dena Loveday and Heather Hesterman. Matthew Brown provided access to the CT scan, the collection of which was funded by the Texas Vertebrate Paleontology Collections. Megan Johnston and Rachel Lyons from Wildcare Australia provided road-killed kangaroos for muscle dissection. We also thank Alex Muir from Logemas for loan of the 3D motion capture system.

Funding

This work was supported by: Australian Government Research Training Program Scholarship and Comparative; ISB Neuromuscular Biomechanics Technical Group Student Grant-in-Aid of Research to LHT; Biotechnology and Biological Sciences Research Council Grant (BB/F000863) to JRH; Journal of Experimental Biology Travelling Fellowship to CPM; Australian Research Council Discovery Project Grant to CJC and TD (DP230101886).

References

Allen, S. P., O. N. Beck, and A. M. Grabowski. 2022. Evaluating the "cost of generating force" hypothesis across frequency in human running and hopping. Cold Spring Harbor Laboratory Press, Cold Spring Harbor.

Baudinette, R. V., and A. A. Biewener. 1998. Young wallabies get a free ride. Nature **395**:653-654.

Baudinette, R. V., B. J. Gannon, W. B. Runciman, S. Wells, and J. B. Love. 1987. Do cardiorespiratory frequencies show entrainment with hopping in the tammar wallaby? Journal of Experimental Biology **129**:251-263.

Baudinette, R. V., G. K. Snyder, and P. B. Frappell. 1992. Energetic cost of locomotion in the tammar wallaby. American Journal of Physiology **262**:771-778.

Bauschulte, C. 1972. Morphologische und biomechanische Grundlagen einer funktionellen Analyse der Muskeln der Hinterextremität (Untersuchung an quadrupeden Affen und Känguruhs). Zeitschrift für Anatomie und Entwicklungsgeschichte **138**:167–214.

Bennett, M. B. 2000. Unifying principles in terrestrial locomotion: do hopping Australian marsupials fit in? Physiological and Biochemical Zoology **73**:726-735.

Bennett, M. B., and G. C. Taylor. 1995. Scaling of elastic strain energy in kangaroos and the benefits of being big. Nature **378**:56-59.

Biewener, A. A. 1989. Scaling body support in mammals: limb posture and muscle mechanics. Science **245**:45-48.

Biewener, A. A. 1990. Biomechanics of mammalian terrestrial locomotion. Science **250**:1097-1103.

Biewener, A. A. 2005. Biomechanical consequences of scaling. Journal of Experimental Biology **208**:1665-1676.

Biewener, A. A., R. M. Alexander, and N. C. Heglund. 1981. Elastic energy storage in the hopping of kangaroo rats (*Dipodomys spectabilis*). Journal of zoology **195**:369-383.

Biewener, A. A., and R. Baudinette. 1995. *In vivo* muscle force and elastic energy storage during steady-speed hopping of tammar wallabies (*Macropus eugenii*). Journal of Experimental Biology **198**:1829-1841.

Biewener, A. A., and R. Blickhan. 1988. Kangaroo rat locomotion: design for elastic energy storage or acceleration? Journal of Experimental Biology **140**:243-255.

Biewener, A. A., C. T. Farley, T. J. Roberts, and M. Temaner. 2004a. Muscle mechanical advantage of human walking and running: implications for energy cost. Journal of Applied Physiology **97**:2266-2274.

Biewener, A. A., D. D. Konieczynski, and R. V. Baudinette. 1998. *In vivo* muscle force-length behavior during steady-speed hopping in tammar wallabies. Journal of Experimental Biology **201**:1681-1694.

Biewener, A. A., C. McGowan, G. M. Card, and R. V. Baudinette. 2004b. Dynamics of leg muscle function in tammar wallabies (*M. eugenii*) during level versus incline hopping. Journal of Experimental Biology **207**:211-223.

Cavagna, G. A., and M. Kaneko. 1977. Mechanical work and efficiency in level walking and running. The Journal of physiology **268**:467-481.

Christensen, B. A., D. C. Lin, M. J. Schwaner, and C. P. McGowan. 2022. Elastic energy storage across speeds during steady-state hopping of desert kangaroo rats (Dipodomys deserti). Journal of Experimental Biology **225**.

Clemente, C. J., and T. J. M. Dick. 2023. How scaling approaches can reveal fundamental principles in physiology and biomechanics. Journal of Experimental Biology **226**.

Dawson, T. J., and C. R. Taylor. 1973. Energetic cost of locomotion in kangaroos. Nature **246**:313-314.

Dawson, T. J., and K. N. Webster. 2010. Energetic characteristics of macropodoid locomotion. Pages 99-108 *in* G. Coulson and M. Eldridge, editors. Macropods: the biology of kangaroos, wallabies and rat-kangaroos. CSIRO Publishing, Collingwood Vic. Australia.

Dick, T. J. M., and C. J. Clemente. 2017. Where have all the giants gone? How animals deal with the problem of size. PLoS biology **15**:e2000473.

Dick, T. J. M., L. K. Punith, and G. S. Sawicki. 2019. Humans falling in holes: adaptations in lower-limb joint mechanics in response to a rapid change in substrate height during human hopping. Journal of the Royal Society interface **16**:20190292.

Heglund, N. C., G. A. Cavagna, and C. R. Taylor. 1982. Energetics and mechanics of terrestrial locomotion. III. Energy changes of the centre of mass as a function of speed and body size in birds and mammals. Journal of Experimental Biology **97**:41-56.

Heglund, N. C., and C. R. Taylor. 1988. Speed, stride frequency and energy cost per stride: how do they change with body size and gait? Journal of Experimental Biology **138**:301-318.

Helgen, K. M., R. T. Wells, B. P. Kear, W. R. Gerdtz, and T. F. Flannery. 2006. Ecological and evolutionary significance of sizes of giant extinct kangaroos. Australian journal of zoology **54**:293-303.

Hopwood, P. R. 1976. The quantitative anatomy of the kangaroo. University of Sydney.

Hopwood, P. R., and R. M. Butterfield. 1976. The musculature of the proximal pelvic limb of the eastern grey kangaroo *Macropus major* (Shaw) *Macropus giganteus* (Zimm). Journal of anatomy **121**:259-277.

Hopwood, P. R., and R. M. Butterfield. 1990. The locomotor apparatus of the crus and pes of the eastern gray kangaroo, *Macropus giganteus*. Australian journal of zoology **38**:397-413.

Janis, C. M., A. M. O'Driscoll, and B. P. Kear. 2023. Myth of the QANTAS leap: perspectives on the evolution of kangaroo locomotion. Alcheringa (Sydney) **ahead-of-print**:1-15.

Kipp, S., A. M. Grabowski, and R. Kram. 2018. What determines the metabolic cost of human running across a wide range of velocities? Journal of Experimental Biology **221**.

Kram, R., and T. J. Dawson. 1998. Energetics and biomechanics of locomotion by red kangaroos (*Macropus rufus*). Comparative Biochemistry and Physiology, Part B **120**:41-49.

Kram, R., and C. R. Taylor. 1990. Energetics of running: a new perspective. Nature **346**:265-267.

Langman, V. A., M. F. Rowe, T. J. Roberts, N. V. Langman, and C. R. Taylor. 2012. Minimum cost of transport in Asian elephants: Do we really need a bigger elephant? Journal of Experimental Biology **215**:1509-1514.

McGowan, C. P., R. V. Baudinette, and A. A. Biewener. 2005. Joint work and power associated with acceleration and deceleration in tammar wallabies (*Macropus eugenii*). Journal of Experimental Biology **208**:41-53.

McGowan, C. P., and C. E. Collins. 2018. Why do mammals hop? Understanding the ecology, biomechanics and evolution of bipedal hopping. Journal of Experimental Biology **221**:jeb161661.

McGowan, C. P., J. Skinner, and A. A. Biewener. 2008. Hind limb scaling of kangaroos and wallabies (superfamily Macropodoidea): implications for hopping performance, safety factor and elastic savings. Journal of anatomy **212**:153-163.

Morgan, D. L., U. Proske, and D. Warren. 1978. Measurements of muscle stiffness and the mechanism of elastic storage of energy in hopping kangaroos. The Journal of physiology **282**:253-261.

O'Connor, S. M., T. J. Dawson, R. Kram, and J. M. Donelan. 2014. The kangaroo's tail propels and powers pentapedal locomotion. Biology Letters **10**:20140381.

Ren, L., C. E. Miller, R. Lair, and J. R. Hutchinson. 2010. Integration of biomechanical compliance, leverage, and power in elephant limbs. Proceedings of the National Academy of Sciences - PNAS **107**:7078-7082.

Seth, A., J. L. Hicks, T. K. Uchida, A. Habib, C. L. Dembia, J. J. Dunne, C. F. Ong, M. S. DeMers, A. Rajagopal, M. Millard, S. R. Hamner, E. M. Arnold, J. R. Yong, S. K. Lakshmikanth, M. A. Sherman, J. P. Ku, and S. L. Delp. 2018. OpenSim: simulating musculoskeletal dynamics and neuromuscular control to study human and animal movement. PLoS computational biology **14**:e1006223.

Smith, N. P., C. J. Barclay, and D. S. Loiselle. 2005. The efficiency of muscle contraction. Progress in Biophysics and Molecular Biology **88**:1-58.

Snelling, E. P., A. A. Biewener, Q. Hu, D. A. Taggart, A. Fuller, D. Mitchell, S. K. Maloney, and R. S. Seymour. 2017. Scaling of the ankle extensor muscle-tendon units and the biomechanical implications for bipedal hopping locomotion in the post-pouch kangaroo *Macropus fuliginosus*. Journal of anatomy **231**:921-930.

Taylor, C. R., N. C. Heglund, and G. M. Maloiy. 1982. Energetics and mechanics of terrestrial locomotion. I. Metabolic energy consumption as a function of speed and body size in birds and mammals. Journal of Experimental Biology **97**:1-21.

Taylor, C. R., N. C. Heglund, T. A. McMahon, and T. R. Looney. 1980. Energetic cost of generating muscular force during running: a comparison of large and small animals. Journal of Experimental Biology **86**:9-18.

Taylor, C. R., K. Schmidt-Nielsen, and J. L. Raab. 1970. Scaling of energetic cost of running to body size in mammals. American Journal of Physiology **219**:1104-1107.

Thompson, S. D., R. E. MacMillen, E. M. Burke, and C. R. Taylor. 1980. The energetic cost of bipedal hopping in small mammals. Nature **287**:223-224.

Thornton, L. H., T. J. M. Dick, M. B. Bennett, and C. J. Clemente. 2022. Understanding Australia's unique hopping species: a comparative review of the musculoskeletal system and locomotor biomechanics in Macropodoidea. Australian journal of zoology **69**:136-157.

Zuntz, N. 1897. Ueber den Stoffverbrauch des Hundes bei Muskelarbeit. Arch. Ges. Physiol. **68**:191-211.

Figures

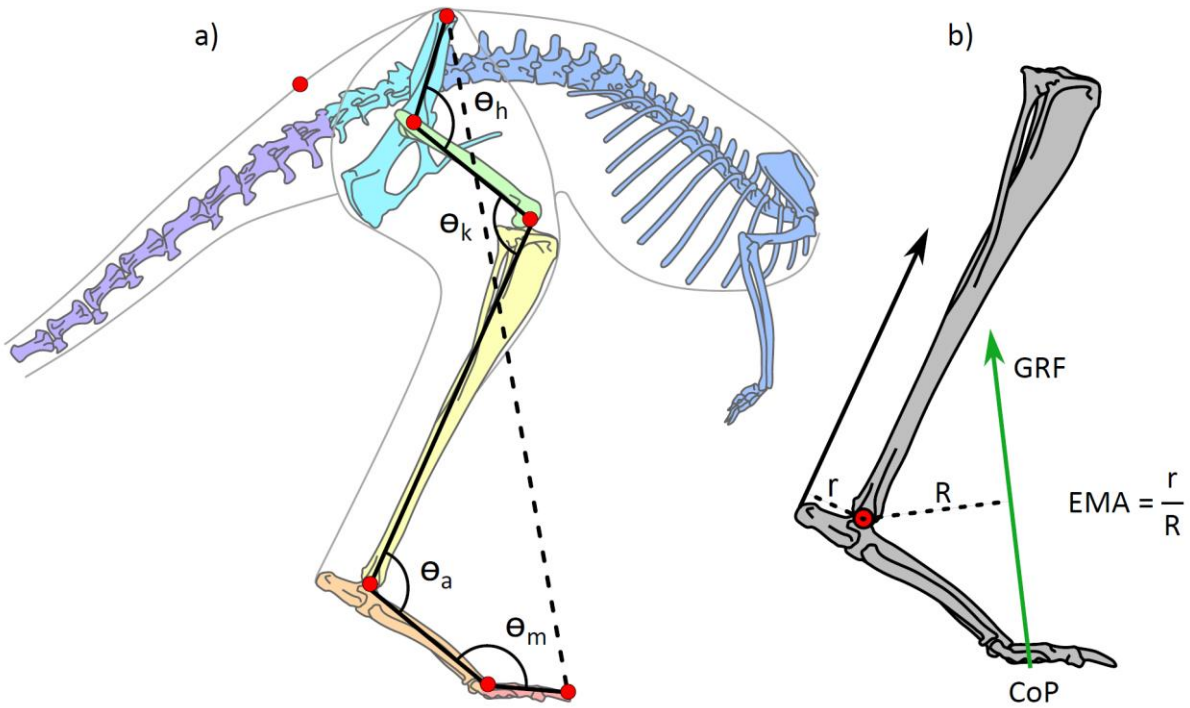

Figure 1: (a) Illustration of the kangaroo model. Total leg length was calculated as the sum of the segment lengths (solid black lines) in the hindlimb and compared to minimum pelvis-to-toe distance (dashed line) to calculate the crouch factor. Joint angles were determined for the hip, h, knee, k, ankle, a, and metatarsophalangeal, m, joints. The model markers (red circles) indicate the position of the reflective markers placed on the kangaroos in the experimental trials and were used to characterize the movement of segments in the musculoskeletal model. (b) Illustration of ankle effective mechanical advantage, EMA, muscle moment arm, r, and external moment arm, R, as the perpendicular distance to the Achilles tendon line of action and ground reaction force (GRF) vector, respectively.

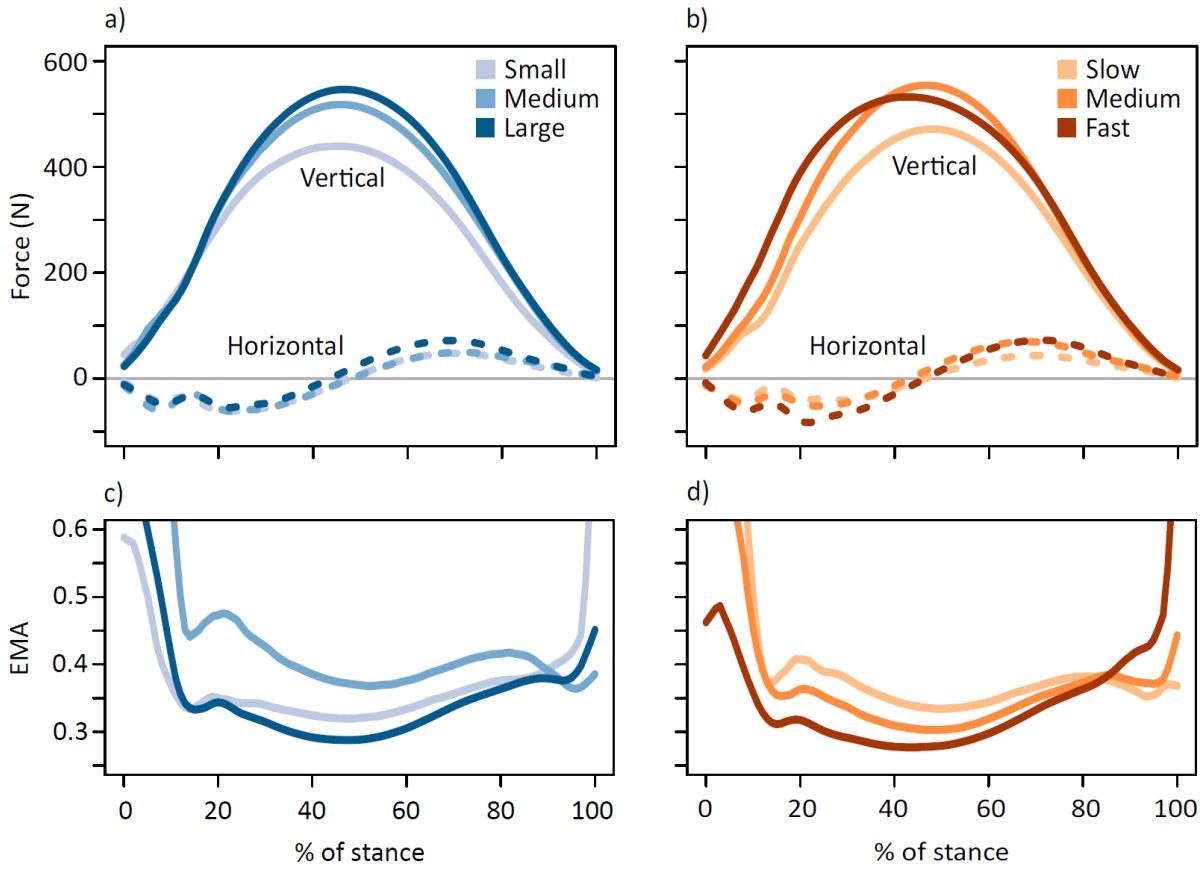

Figure 2: Horizontal (dashed lines) and vertical (solid lines) components of the ground reaction force (GRF) (a) coloured by body mass subsets (small 17.6±2.96 kg, medium 21.5±0.74 kg, large 24.0±1.46 kg) and (b) coloured by speed subsets (slow 2.52±0.25 m s^{-1}, medium 3.11±0.16 m s^{-1}, fast 3.79±0.27 m s^{-1}). In (a) and (b) the medial-lateral component of the GRF is not shown as it remained close to zero, as expected for animals moving in a straight-line path. Lower panels show average time-varying EMA for the ankle joint subset by (c) body mass and (d) speed.

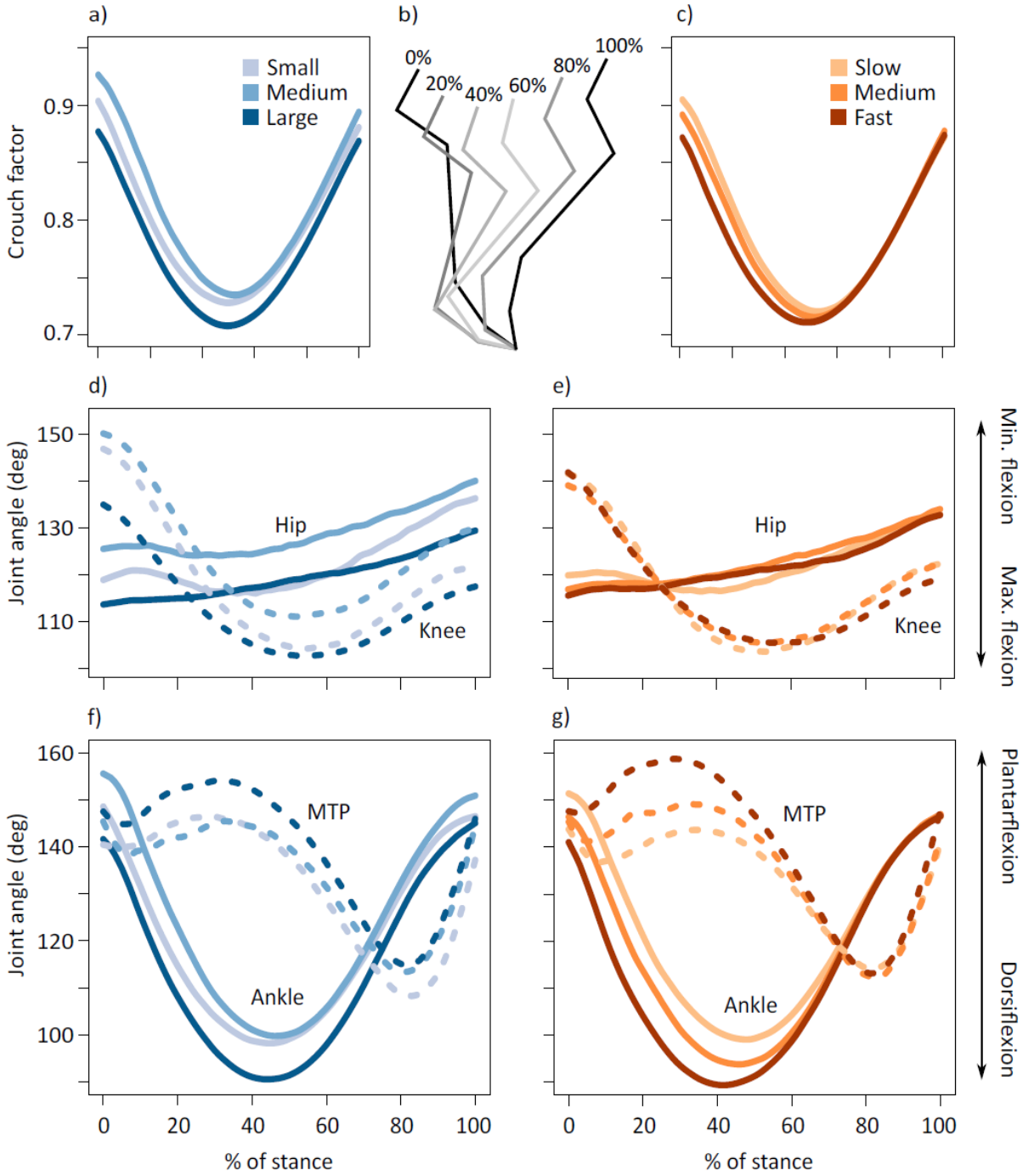

Figure 3: Average time-varying crouch factor of the kangaroo hindlimb grouped by (a) body mass and (c) speed. Position of the limb segments during % stance intervals (b). Average time-varying joint angles for the hip (solid lines) and knee (dashed lines) displayed for kangaroos grouped by (d) body mass and (e) speed. Average time-varying joint angles for the ankle (solid lines) and metatarsophalangeal (MTP) joints (dashed lines) displayed for kangaroos grouped by (f) body mass and (g) speed. Body mass subsets: small 17.6±2.96 kg, medium 21.5±0.74 kg, large 24.0±1.46 kg. Speed subsets: slow 2.52±0.25 m s^{-1}, medium 3.11±0.16 m s^{-1}, fast 3.79±0.27 m s^{-1}.

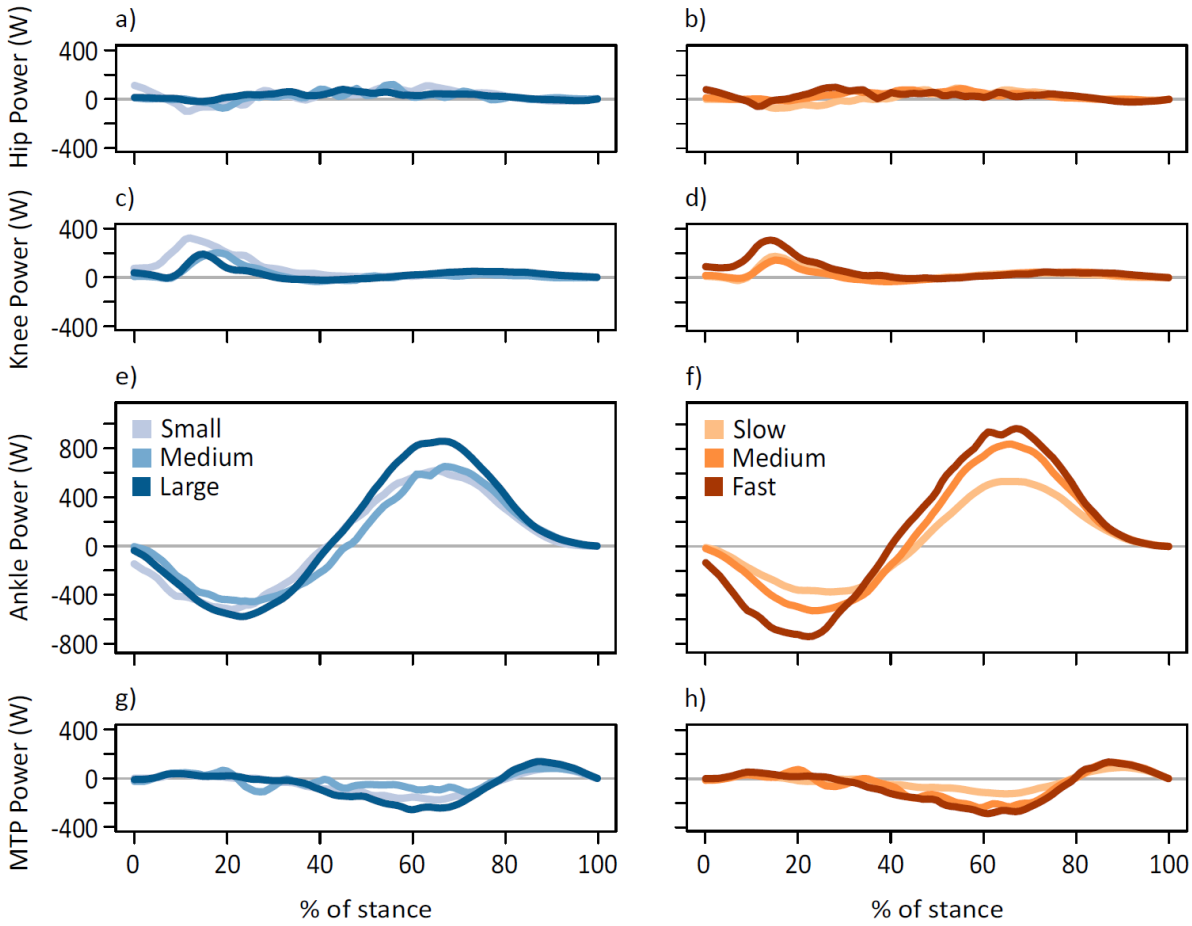

Figure 4: Average time-varying joint powers for the hip (a,b), knee (c, d), ankle (e, f), and MTP (g, h) displayed for kangaroos grouped by body mass (a, c, e, g) and speed (b, d, f, h). Body mass subsets: small 17.6±2.96 kg, medium 21.5±0.74 kg, large 24.0±1.46 kg. Speed subsets: slow 2.52±0.25 m s^{-1}, medium 3.11±0.16 m s^{-1}, fast 3.79±0.27 m s^{-1}.

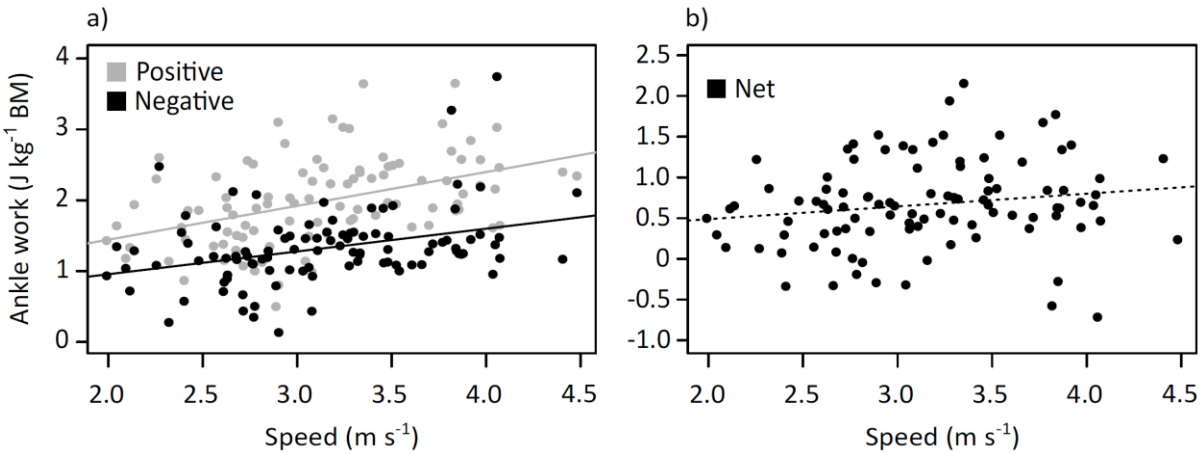

Figure 5: Variation with speed of (a) positive and negative ankle work, and (b) net ankle work.

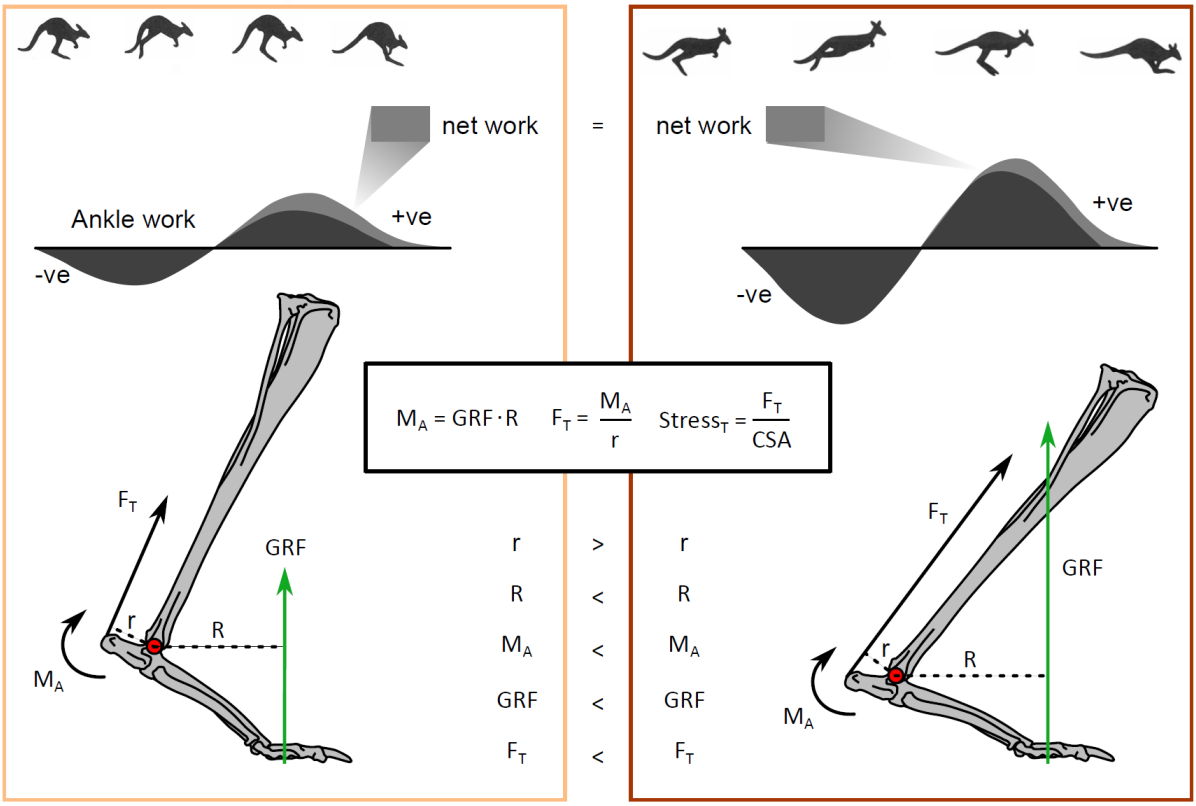

Figure 6: How the relationship between posture and speed is proposed to change tendon stress. Forces are not to scale and joint angles are exaggerated for illustrative clarity. A slow hop (left panel) compared to a fast hop (right panel). The increase in ground reaction force (GRF) with speed, while a more crouched posture changes the muscle moment arm, r, and external moment arm, R, which allows the ankle to do more negative work (storing elastic potential energy in the tendons due to higher tendon stresses), without increasing net work, and thereby metabolic cost.

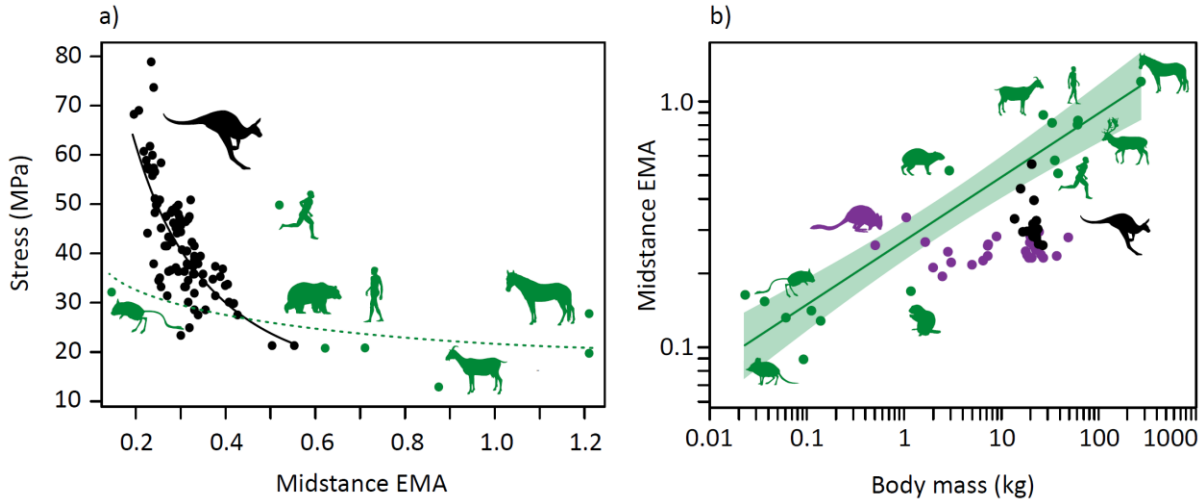

Figure 7: (a) Relationship between ankle effective mechanical advantage, EMA, at midstance and Achilles tendon stress (stress = 11.6 $EMA^{-1.04}$, R^2=0.593) (black), with other mammals (green). (b) Scaling of mean ankle EMA at midstance for each individual kangaroo against body mass (black), with data for a wider range of macropods (purple) (Bennett and Taylor 1995), and other mammals (green, EMA = 0.269 $M^{0.259}$, shaded area 95% confidence interval) (Biewener 1990) shown.

Supplementary Results

Stride parameters

Preferred hopping speed ranged from 1.99 to 4.48 m s^{-1}. Larger kangaroos tended to hop at slightly faster speeds (B=0.048, SE=0.018, P=0.009, R^2=0.057), and due to this weak relationship between body mass and speed, both variables were considered in multiple linear regression models to determine their relative effects on the outcome measures (see Table 1).

Faster speeds were associated with a greater magnitude of acceleration in the braking period of the stance phase, i.e. minimum horizontal acceleration and maximum vertical acceleration (Suppl. Fig. 1a). There was no significant relationship between body mass and acceleration; however, there was a significant interaction between body mass and speed on maximum vertical acceleration, whereby smaller kangaroos had a greater change in vertical acceleration between slower and faster hopping speeds than larger kangaroos (Table 1).

Body mass and speed had different effects on ground contact duration (Table 1). There was a slight increase in contact duration in larger kangaroos. A stronger, opposing relationship was found with speed, and as speed increased, contact duration decreased. The relatively tight correlation between contact duration and hopping speed (R^2=0.73) could prove useful for predicting speed when contact duration can be accurately measured. In Suppl. Fig. 1b we combined our data with red kangaroo data from Kram and Dawson (1998) to extend the predictive range of both studies.

Larger kangaroos hopped with longer strides and lower frequencies than smaller kangaroos (Table 1), and stride length also increased with speed (Suppl. Fig. 1c). We found a significant decrease in stride frequency with mass and an increase with speed, if we did not consider the interaction term (Suppl. Fig. 1d). However, a significant interaction between body mass and speed suggests that larger kangaroos relied more on increases in stride frequency to increase hopping speed compared to smaller kangaroos (Table 1).

Ground reaction forces

It is commonly assumed that the GRF is vertical and at a maximum at midstance or 50% of stance (Bennett and Taylor 1995, Kram and Dawson 1998, McGowan et al. 2008, Snelling et al. 2017) but our results suggest it occurred earlier, at 42.9±26.9% of stance, and the wide range suggests such assumptions should be used with caution.

Kinematics and posture

Kangaroos were maximally crouched at midstance, with crouch factor (CF) reaching a minimum at 50.1±4.2% of stance. Crouch factor (CF) at initial ground contact decreased at faster speeds,

although the limb was similarly flexed during midstance (P=0.295). Consequently, CF changed less at faster speeds than slower speeds.

Larger kangaroos had lower hip and knee ranges of motion (ROM) compared to smaller kangaroos (Fig. 3d; Suppl. Table 3). In the distal hindlimb, ankle ROM increased with body mass, largely owing to an increase in dorsiflexion at midstance (Fig. 3f; Suppl. Table 3). The ROM of the MTP joint did not change with body mass; however, there was both an increase in plantarflexion and a decrease in dorsiflexion, resulting in a shift to larger MTP angles with mass (Fig. 3f; Suppl. Table 3).

Joint moments

Despite the small changes in joint rotation in the proximal hindlimb, we detected a decrease in magnitude of the dimensionless hip extensor and knee flexor moments with mass (Suppl. Fig. 4a, Suppl. Table 4), and an increase in magnitude of both joint moments with speed during the braking period of stance (Suppl. Fig. 4b). Maximum hip extensor moment and knee flexor moment were significantly influenced by the interaction between body mass and speed, suggesting that larger kangaroos increased the magnitude of the moments at a faster rate with speed compared to smaller kangaroos.

Joint work and power

The MTP was the only joint which did predominantly negative work. The MTP did more negative work with speed, while net MTP work decreased with both mass and speed (Suppl. Fig. 5g,h; Suppl. Fig. 6g,h; Suppl. Table 6). The MTP transition from negative work to positive work at ~80% stance, as the back of the foot started to leave the ground. Conversely, the knee did almost no negative work, and the hip did very little (Fig. 4; Suppl. Fig. 5; Suppl. Fig. 6). Net work slightly increased with mass and speed in the hip, while at the knee, net work increased only with speed (Suppl. Table 6).

Supplementary Videos

Suppl Video 1: A red kangaroo hopping on the force plate during data collection.

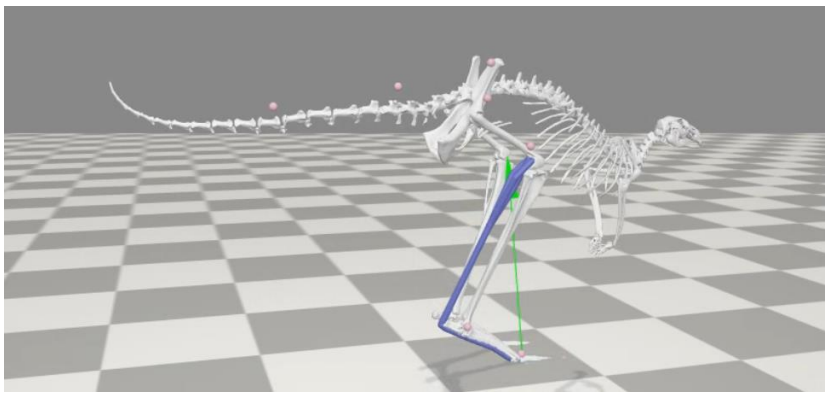

Suppl Video 2: Diving the musculoskeletal model with a recorded hopping trial. The gastrocnemius and plantaris muscle-tendon unit (achilles) is shown in blue. The GRF appears in green. Markers associating the recorded kangaroos with the model are in pink.

Supplementary Figures

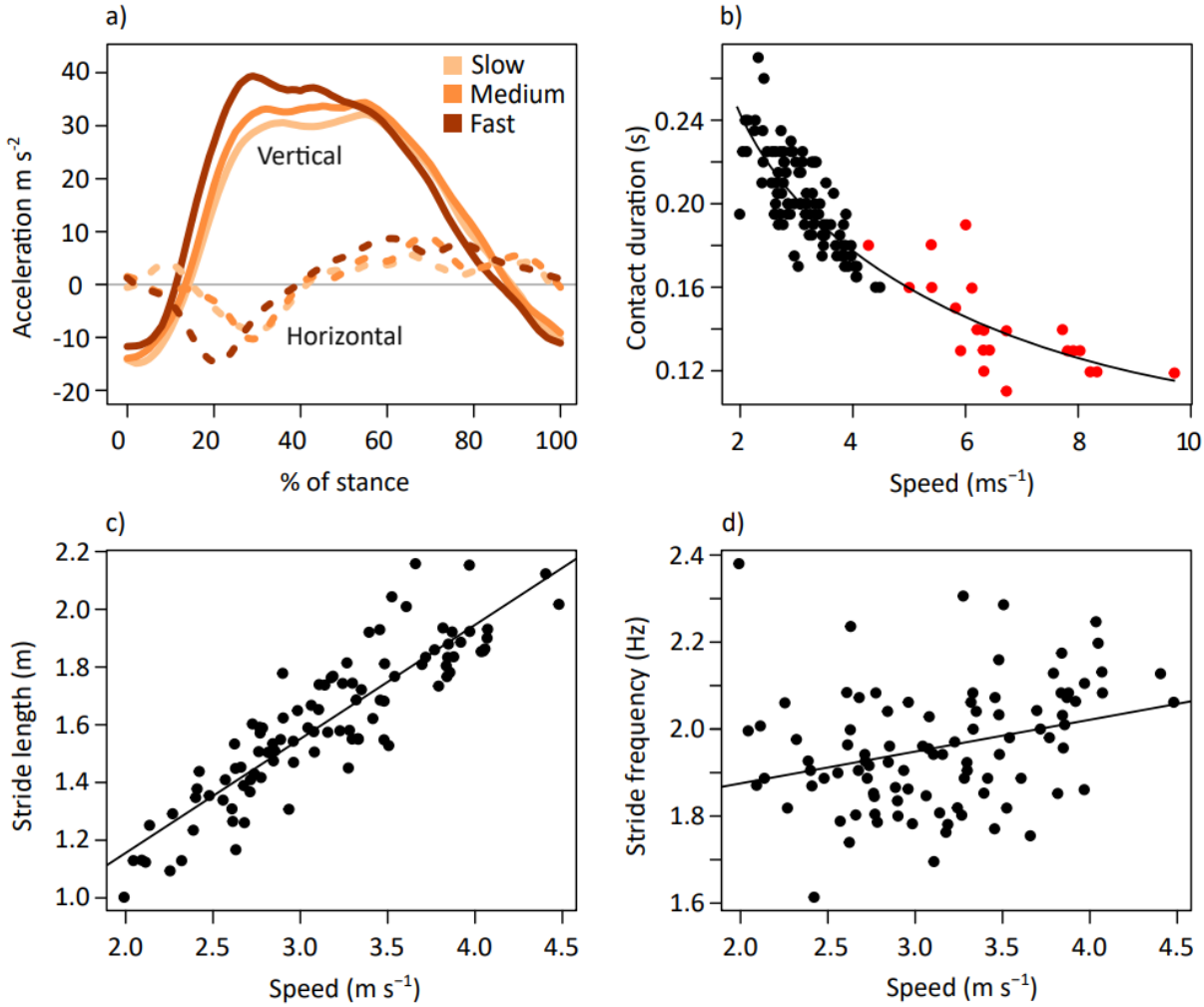

Suppl Figure 1: a) Mean vertical and horizontal components of whole body acceleration for kangaroos in the slow, medium and fast subsets (respectively: 2.52±0.25 m s^{-1}, 3.11±0.16 m s^{-1}, 3.79±0.27 m s^{-1}). (b) Ground contact duration across hopping speeds from current study (black circles) and for red kangaroos reported in Kram and Dawson (1998) (red circles). Regression equation: $t_c = 0.342\text{speed}^{-0.477}$ where t_c is contact duration and s is hopping speed. (c) Relationship between stride length and speed, and (d) stride frequency and speed.

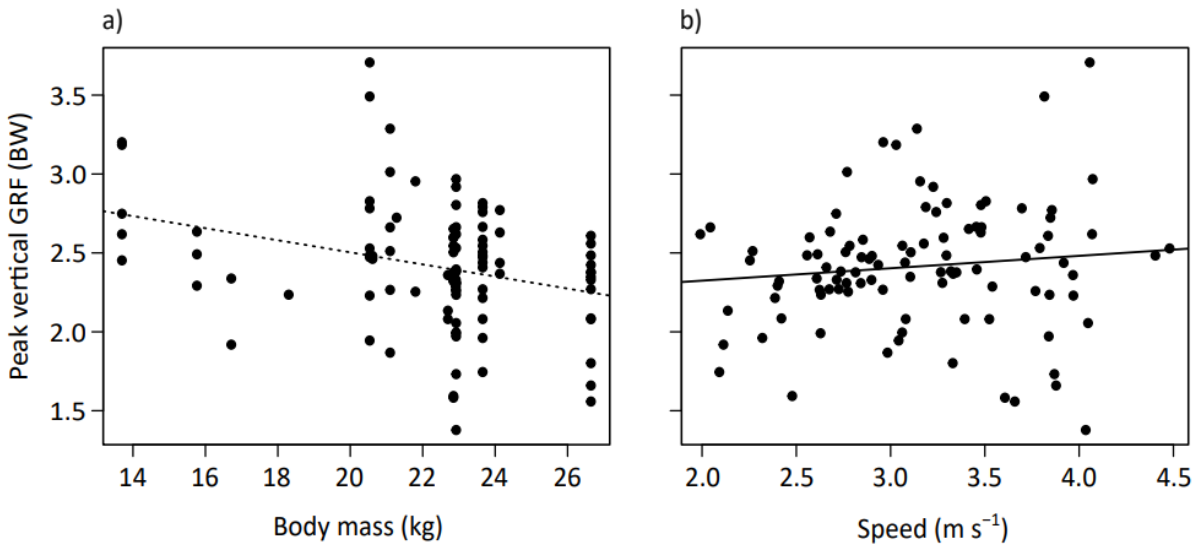

Suppl Figure 2: (a) Relationship between peak vertical GRF as a multiple of body weight (BW) with body mass and (b) with speed. Dotted line is insignificant and solid line is significant, see Table 2 for interaction.

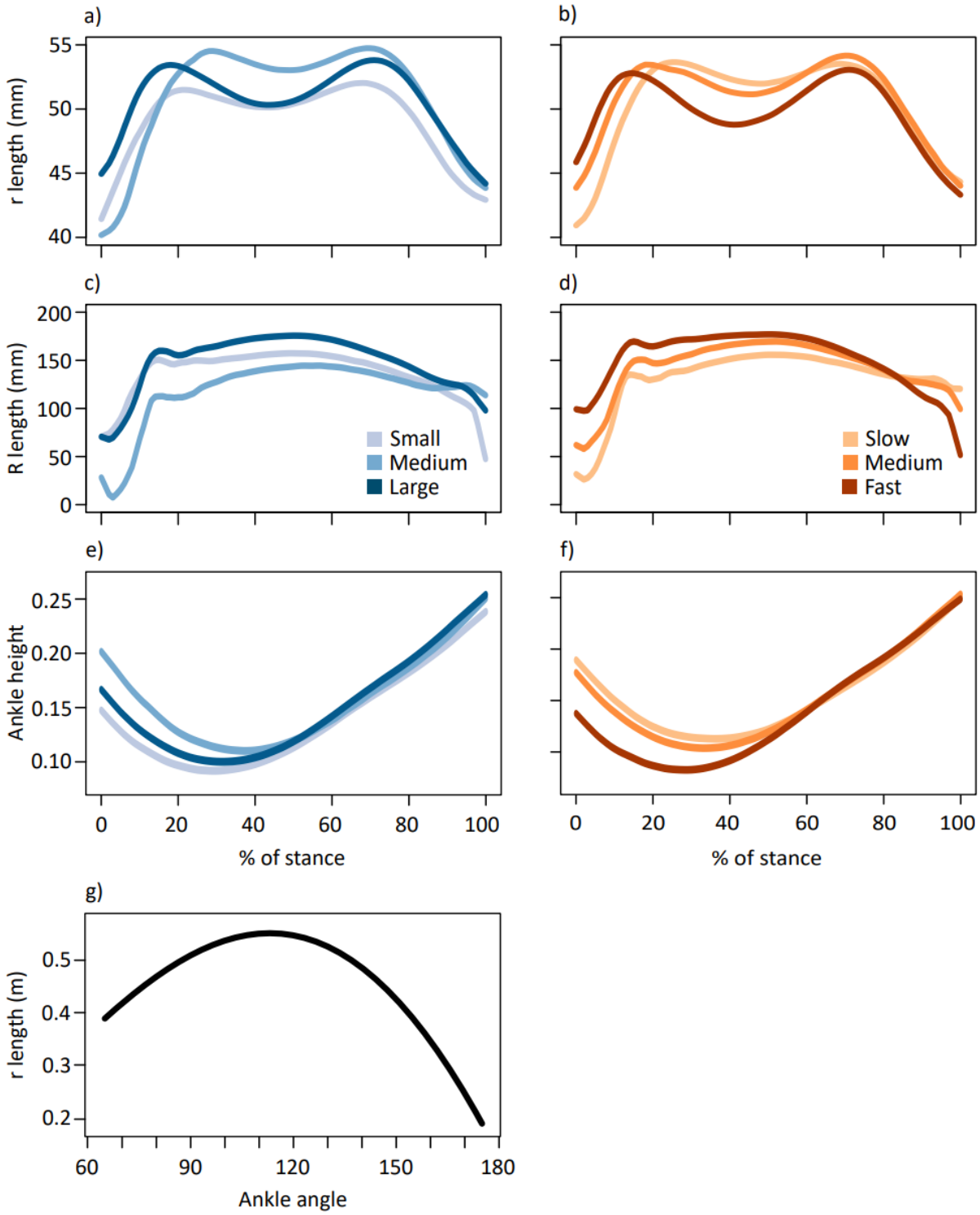

Suppl Figure 3: Average time-varying muscle moment arm, *r*, grouped by (a) body mass and (b) speed; external moment arm, *R*, grouped by (c) body mass and (d) speed. Vertical displacement of the ankle marker from the ground throughout stance grouped by (e) body mass and (f) speed. Ankle angles and corresponding r arm length (g). Body mass subsets: small 17.6±2.96 kg, medium 21.5±0.74 kg, large 24.0±1.46 kg. Speed subsets: slow 2.52±0.25 m s^{-1}, medium 3.11±0.16 m s^{-1}, fast 3.79±0.27 m s^{-1}.

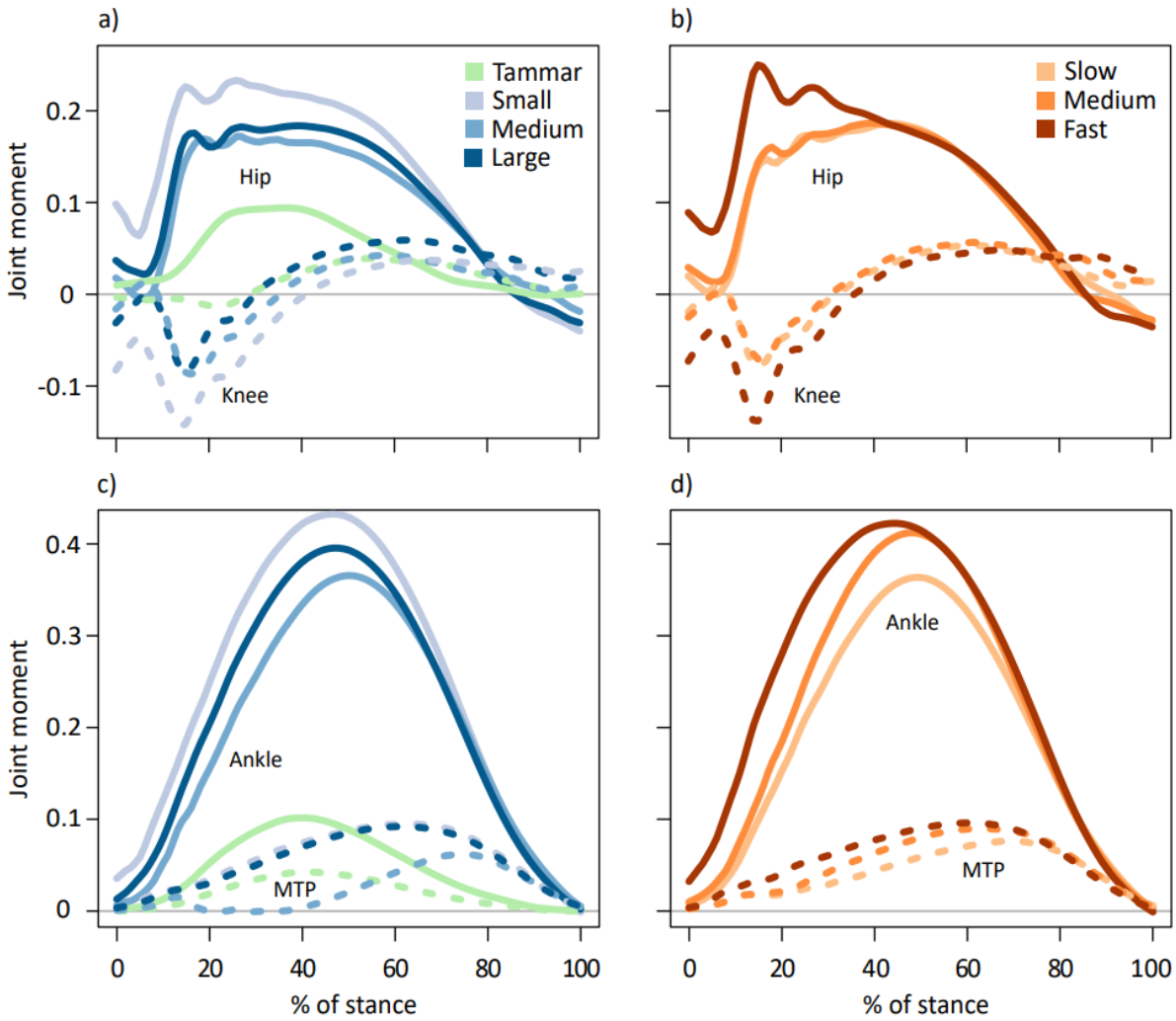

Suppl Figure 4: Average time-varying net joint moments (dimensionless, as moments were divided by body weight * leg length) for the hip (solid lines) and knee (dotted lines) displayed for kangaroos grouped by (a) body mass and (b) speed. Average time-varying net joint moments (dimensionless) for the ankle (solid lines) and metatarsophalangeal (MTP; dotted lines) joints displayed for kangaroos grouped by (c) body mass and (d) speed. Data for tammar wallabies was also included (McGowan et al. 2005) in green. Peak ankle moment occurred at 47.37±4.91 % of the stance phase. Positive values represent extensor moments and negative values represent flexor moments. Body mass subsets: small 17.6±2.96 kg, medium 21.5±0.74 kg, large 24.0±1.46 kg. Speed subsets: slow 2.52±0.25 m s^{-1}, medium 3.11±0.16 m s^{-1}, fast 3.79±0.27 m s^{-1}.

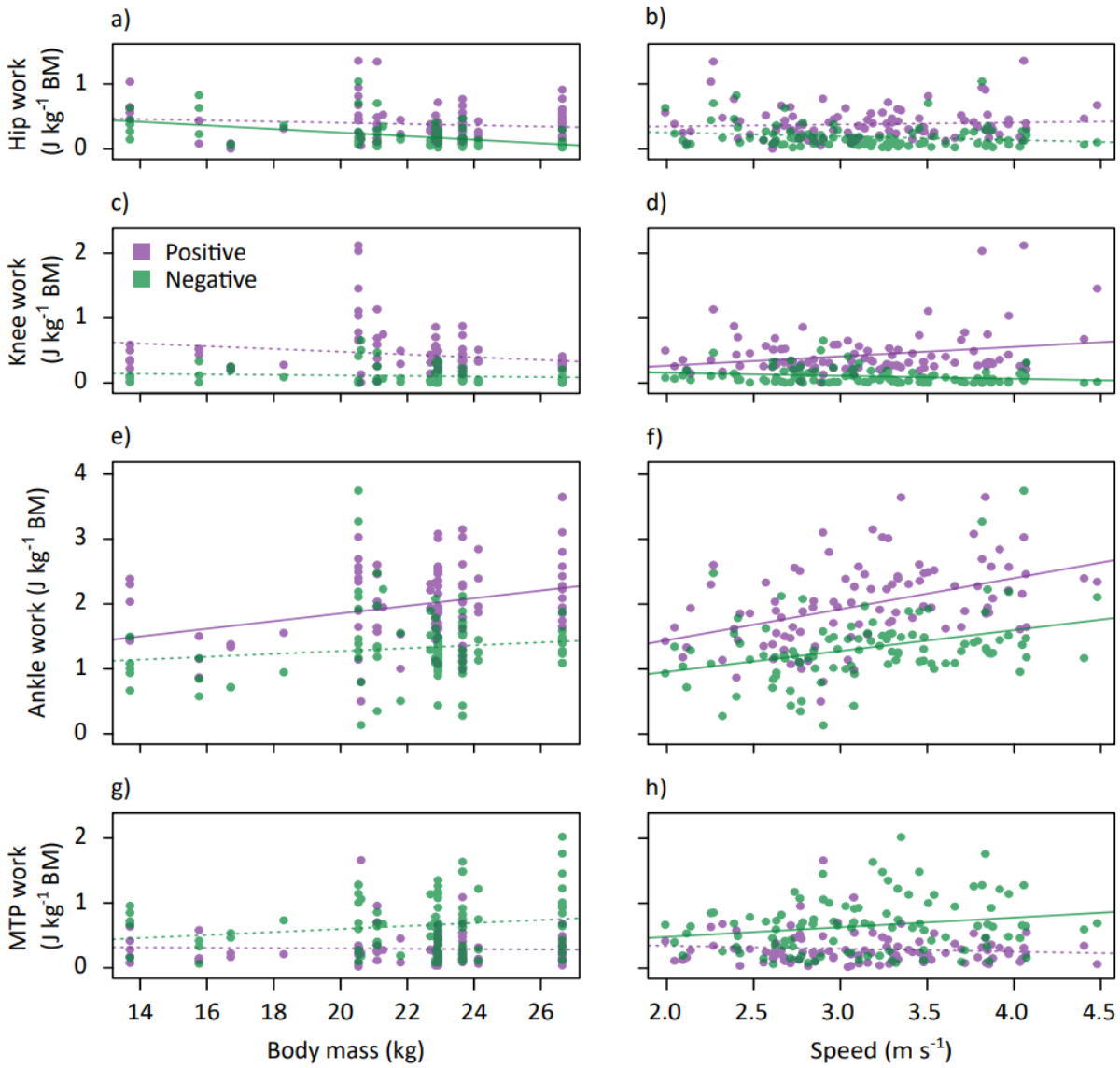

Suppl Figure 5: Positive (purple) and negative (green) joint work over stance for the hip, knee, ankle and MTP plotted against body mass (a,c,e,g) and speed (b,d,f,h). Solid lines represent significant trends, dotted lines are not significant (see Suppl Table 6).

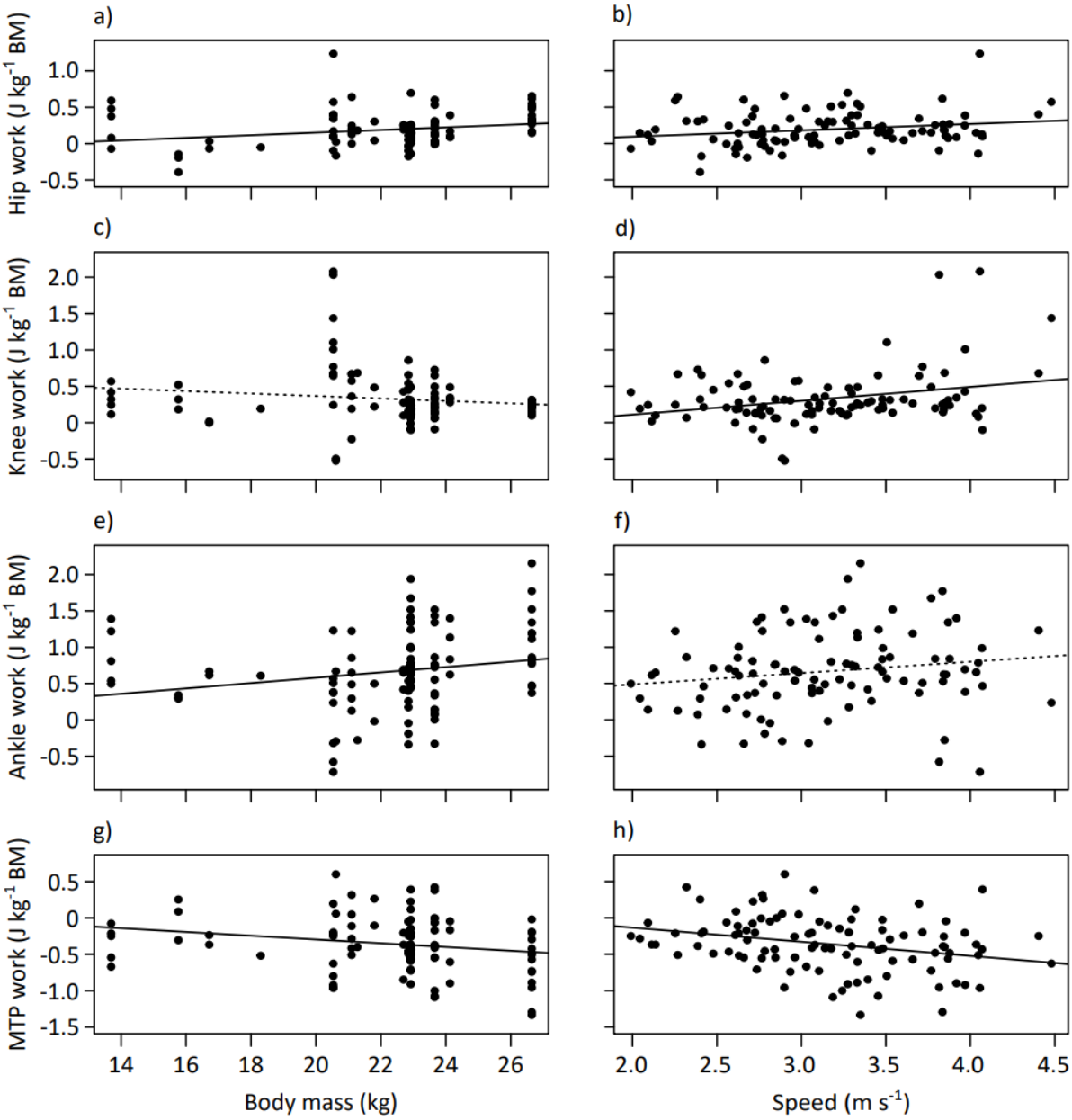

Suppl Figure 6: Net joint work for the hip, knee, ankle and MTP joint over stance plotted against body mass (a,c,e,g) and speed (b,d,f,h). Solid lines represent significant trends, dotted lines are not significant (see Suppl Table 6).

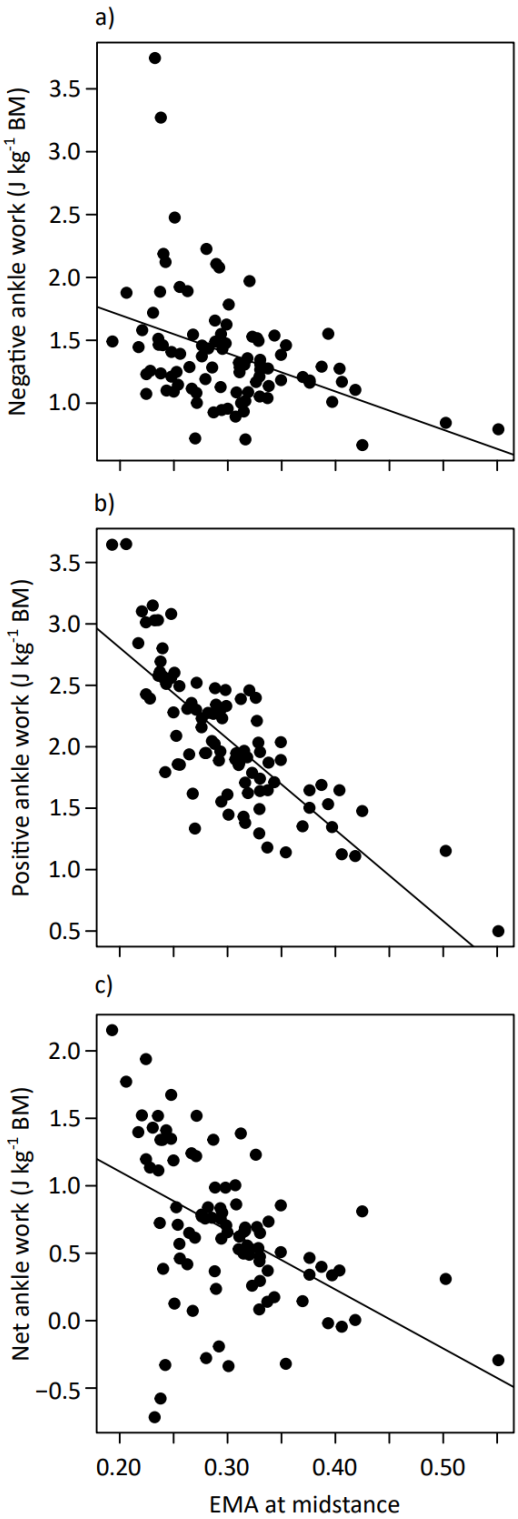

Suppl Figure 7: Negative (a) (B=-3.04, SE=0.75, P<0.001, R^2=0.155), positive (b) (B=-7.42, SE=0.61, P<0.001, R^2=0.622), and net ankle work (c) (B=-4.37, SE=0.84, P<0.001, R^2=0.230) plotted against EMA at 50% of stance.

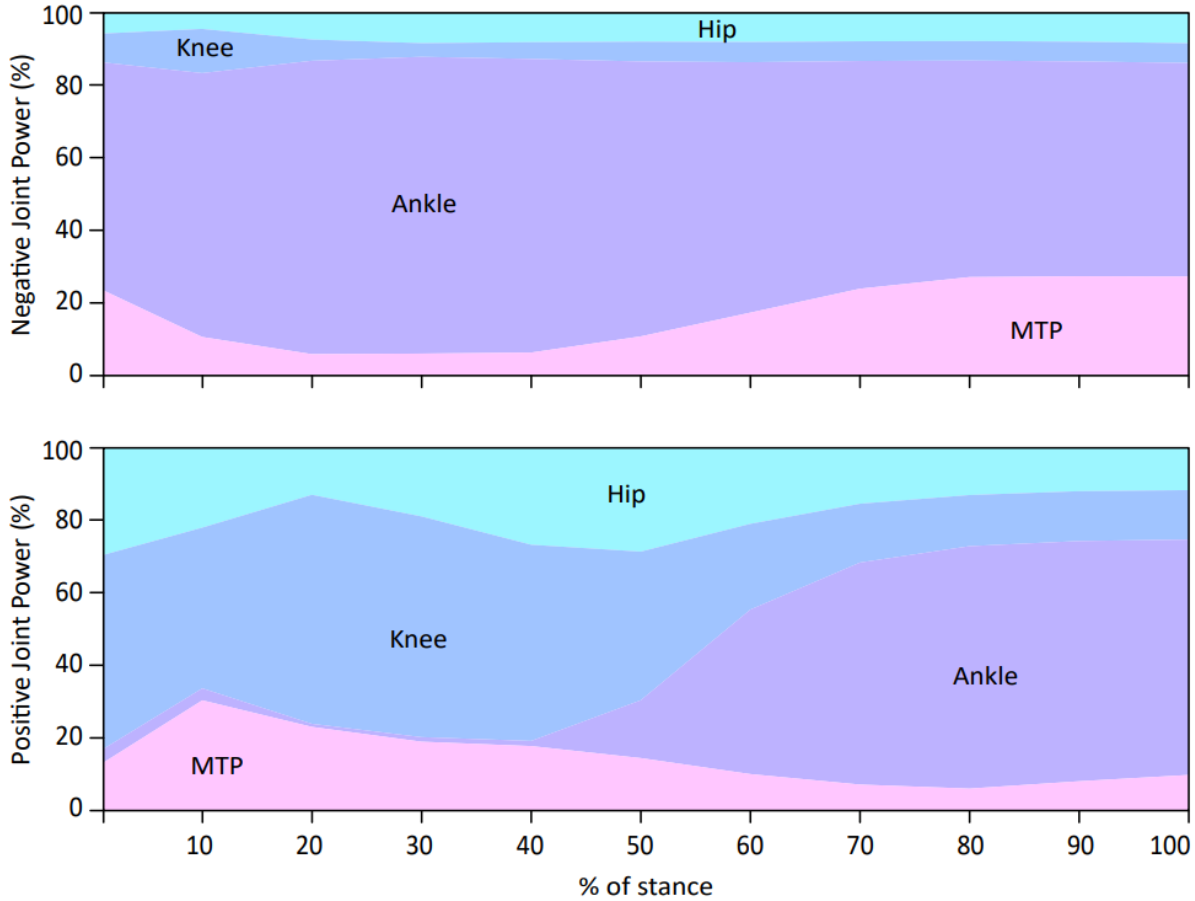

Suppl Figure 8: Mean instantaneous positive (top panel) and negative (bottom panel) power for each hindlimb joint expressed as a percentage of total limb power (sum of instantaneous joint powers). Means were calculated at 10% stance intervals.

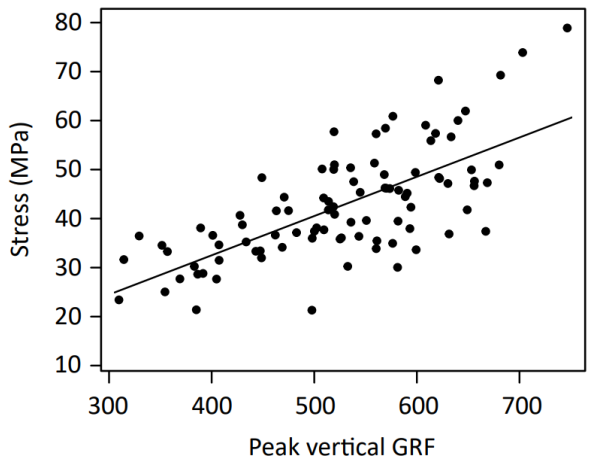

Suppl Figure 9: Peak vertical ground reaction force (GRF) plotted against tendon stress (B=0.080, SE=0.009, P<0.001, R^2=0.486).

Tables

Suppl Table 1: Stride parameter multiple linear regression results as slopes, standard errors and P-values. Models with a significant interaction are displayed in full, and as a simplified model without the interaction term included (marked *). The fit of the model is represented by R^2 and relationships are considered significant at P<0.05.

	Interaction			Body mass			Speed			R^2
	β	SE	P	β	SE	P	β	SE	P	
Maximum vertical acceleration (m s^{-2})	-1.19	0.567	0.038	2.72	1.64	0.100	32.5	12.5	0.011	0.190
Maximum vertical acceleration (m s^{-2})*				-0.673	0.294	0.024	6.32	1.60	0.000	0.152
Minimum vertical acceleration (m s^{-2})				0.221	0.208	0.290	-0.268	1.13	0.814	0.012
Maximum horizontal acceleration (m s^{-2})				-0.036	0.296	0.903	0.159	1.61	0.922	0.000
Minimum horizontal acceleration (m s^{-2})				0.407	0.370	0.275	-6.05	2.02	0.003	0.087
Contact duration (ms)				2.87	0.393	0.000	-34.2	2.12	0.000	0.735
Stride length (m)				0.014	0.004	0.001	0.376	0.020	0.000	0.815
Stride frequency (Hz)	0.022	0.008	0.007	-0.082	0.023	0.001	-0.392	0.180	0.032	0.303
Stride frequency (Hz)*				-0.019	0.004	0.000	0.102	0.023	0.000	0.245

Suppl Table 2: Ground reaction force and centre of pressure (CoP) multiple linear regression results as slopes, standard errors and P-values. Models with a significant interaction are displayed in full, and as a simplified model without the interaction term included (marked *). The fit of the model is represented by R^2 and relationships are considered significant at P<0.05.

	Interaction			Body mass			Speed			R^2
	β	SE	P	β	SE	P	β	SE	P	
Normalised peak GRF (BW)	-0.055	0.024	0.026	0.111	0.070	0.117	1.34	0.535	0.014	0.172
Normalised peak GRF (BW)*				-0.045	0.013	0.001	0.142	0.068	0.040	0.128
Peak vertical GRF (N)	-11.5	5.31	0.032	47.9	15.4	0.002	281	117	0.019	0.332
Peak vertical GRF (N)*				15.0	2.76	0.000	28.4	14.9	0.060	0.299
Peak braking GRF (N)	4.87	2.04	0.019	-14.8	5.90	0.014	-130	45.0	0.005	0.218
Peak braking GRF (N)*				-0.917	1.07	0.392	-23.2	5.76	0.000	0.172
Peak propulsive GRF (N)				2.03	0.818	0.015	21.5	4.42	0.000	0.285
CoP location at midstance (mm)				-0.123	1.54	0.937	-15.2	8.34	0.071	0.036
CoP location at midstance corrected for phalanx size (mm)				-0.437	17.0	0.980	-62.7	91.9	0.497	0.005

Suppl Table 3: Crouch factor (CF) and kinematics multiple linear regression results as slopes, standard errors and P-values. Models with a significant interaction are displayed in full, and as a simplified model without the interaction term included (marked *). The fit of the model is represented by R^2 and relationships are considered significant at P<0.05.

	Interaction			Body mass			Speed			R^2
	β	SE	P	β	SE	P	β	SE	P	
Maximum CF				-2.19	1.07	0.043	-15.8	5.74	0.007	0.122
Minimum CF				-2.45	0.885	0.007	-1.53	4.76	0.749	0.064
Change in CF				0.256	0.661	0.699	-14.2	3.55	0.000	0.129
Pelvis pitch ROM (deg)	0.935	0.298	0.002	-2.60	0.862	0.003	-19.9	6.58	0.003	0.100
Pelvis pitch ROM (deg)*				0.066	0.159	0.677	0.534	0.858	0.535	0.008
Hip ROM (deg)				-0.488	0.212	0.024	0.490	1.15	0.670	0.052
Minimum hip flexion (deg)				-0.655	0.315	0.040	0.703	1.70	0.681	0.043
Maximum hip flexion (deg)				-0.167	0.260	0.520	0.213	1.40	0.880	0.004
Knee ROM (deg)	-1.31	0.520	0.013	2.88	1.50	0.058	28.6	11.5	0.014	0.154
Knee ROM (deg)*				-0.850	0.272	0.002	-0.120	1.47	0.935	0.098
Minimum knee flexion (deg)	-1.72	0.649	0.010	3.76	1.88	0.048	39.5	14.3	0.007	0.162
Minimum knee flexion (deg)*				-1.13	0.34	0.001	1.95	1.84	0.294	0.101
Maximum knee flexion (deg)				-0.277	0.265	0.299	2.07	1.43	0.152	0.026
Ankle ROM (deg)				1.02	0.166	0.000	1.63	0.899	0.073	0.339
Peak ankle plantarflexion (deg)				-0.173	0.240	0.474	-3.87	1.30	0.004	0.104
Peak ankle dorsiflexion (deg)				-1.19	0.198	0.000	-5.49	1.07	0.000	0.466
MTP ROM (deg)				-0.098	0.259	0.707	7.16	1.40	0.000	0.219
Peak MTP plantarflexion (deg)				0.875	0.306	0.005	5.64	1.65	0.001	0.216
Peak MTP dorsiflexion (deg)				0.973	0.221	0.000	-1.52	1.20	0.205	0.166

Suppl Table 4: Multiple linear regression results of dimensionless peak joint moments as slopes, standard errors and P-values. Models with a significant interaction are displayed in full, and as a simplified model without the interaction term included (marked *). The fit of the model is represented by R^2 and relationships are considered significant at P<0.05.

	Interaction			Body mass			Speed			R^2
	β	SE	P	β	SE	P	β	SE	P	
Hip extensor moment	-0.020	0.006	0.001	0.049	0.018	0.007	0.525	0.136	0.000	0.268
Hip extensor moment*				-0.009	0.003	0.010	0.079	0.018	0.000	0.184
Knee extensor moment				0.000	0.001	0.766	0.003	0.008	0.721	0.003
Knee flexor moment	0.020	0.005	0.000	-0.048	0.015	0.002	-0.487	0.116	0.000	0.264
Knee flexor moment*				0.008	0.003	0.007	-0.060	0.015	0.000	0.158
Ankle extensor moment				-0.004	0.004	0.256	0.043	0.020	0.036	0.048
MTP extensor moment				-0.001	0.002	0.767	0.000	0.013	0.986	0.001

Suppl Table 5: Tendon stress and EMA multiple linear regression results as slopes, standard errors and P-values. Models with a significant interaction are displayed in full, and as a simplified model without the interaction term included (marked *). The fit of the model is represented by R^2 and relationships are considered significant at P<0.05.

	Interaction			Body mass			Speed			R^2
	β	SE	P	β	SE	P	β	SE	P	
r at midstance (mm)				-0.063	0.088	0.477	-1.88	0.474	0.000	0.173
R at midstance (mm)				3.49	1.03	0.001	-0.93	5.59	0.869	0.117
EMA at midstance				-6.64	1.98	0.001	-11.0	10.7	0.310	0.142
Peak tendon stress (MPa)				1.03	0.385	0.008	5.61	2.08	0.008	0.168
Normalised peak tendon stress				-0.048	0.018	0.008	0.258	0.096	0.008	0.107
Peak tendon stress timing %stance				-0.151	0.154	0.328	-3.13	0.831	0.000	0.159
Ankle height from ground (mm)				-0.298	0.706	0.674	-23.0	3.81	0.000	0.295

Suppl Table 6: Joint net positive, negative and net work simple linear regression (lm(joint work ~ mass), lm(joint work ~ speed)) results as slopes, standard errors and P-values. Work is normalised by body mass (BM). The fit of the model is represented by R^2 and relationships are considered significant at P<0.05.

	Body mass				Speed			
	β	SE	P	R^2	β	SE	P	R^2
Hip pos	-0.010	0.008	0.238	0.014	0.030	0.044	0.497	0.005
Hip neg	-0.027	0.005	0.000	0.225	-0.058	0.031	0.066	0.034
Hip net	0.018	0.007	0.018	0.055	0.087	0.041	0.034	0.045
Knee pos	-0.021	0.011	0.052	0.038	0.145	0.057	0.013	0.061
Knee neg	-0.004	0.004	0.267	0.013	-0.046	0.020	0.026	0.050
Knee net	-0.017	0.012	0.169	0.019	0.191	0.064	0.003	0.084
Ankle pos	0.059	0.019	0.003	0.087	0.478	0.097	0.000	0.197
Ankle neg	0.022	0.017	0.200	0.017	0.321	0.087	0.000	0.122
Ankle net	0.037	0.017	0.037	0.044	0.156	0.095	0.102	0.027
MTP pos	-0.003	0.008	0.743	0.001	-0.046	0.043	0.286	0.012
MTP neg	0.023	0.014	0.089	0.029	0.149	0.073	0.044	0.041
MTP net	-0.026	0.012	0.035	0.045	-0.194	0.064	0.003	0.086

Suppl Table 7: Positive, negative and net joint work multiple linear regression results as slopes, standard errors and P-values. Work is normalised by body mass (BM). Models with a significant interaction are displayed in full, and as a simplified model without the interaction term included (marked *). The fit of the model is represented by R^2 and relationships are considered significant at $P<0.05$.

Joint work (J kg^{-1} BM)	Interaction			Body mass			Speed			R^2
	β	SE	P	β	SE	P	β	SE	P	
Hip positive				0.046	0.045	0.307	-0.012	0.008	0.161	0.025
Hip negative				-0.021	0.029	0.472	-0.026	0.005	0.000	0.229
Hip net				0.067	0.042	0.110	0.015	0.008	0.058	0.080
Knee positive	-0.072	0.020	0.000	1.766	0.431	0.000	0.175	0.057	0.003	0.241
Knee positive*				0.187	0.057	0.002	-0.030	0.011	0.006	0.133
Knee negative				-0.043	0.021	0.045	-0.002	0.004	0.570	0.053
Knee net	-0.073	0.022	0.002	1.818	0.491	0.000	0.179	0.064	0.007	0.219
Knee net*				0.230	0.064	0.001	-0.028	0.012	0.021	0.133
Ankle positive				0.424	0.099	0.000	0.039	0.018	0.038	0.232
Ankle negative	-0.080	0.032	0.015	2.052	0.707	0.005	0.234	0.093	0.013	0.176
Ankle negative*				0.311	0.091	0.001	0.007	0.017	0.671	0.123
Ankle net	0.122	0.033	0.000	-2.551	0.732	0.001	-0.315	0.096	0.001	0.173
Ankle net*				0.112	0.097	0.250	0.031	0.018	0.084	0.057
MTP positive				-0.045	0.044	0.312	0.000	0.008	0.956	0.012
MTP negative				0.125	0.075	0.101	0.017	0.014	0.217	0.056
MTP net				-0.170	0.066	0.011	-0.018	0.012	0.149	0.106

Suppl Table 8: The mean and standard deviation of joint work for all trials. Positive, negative and net work is presented for each joint.

Joint work (J kg^{-1} BM)	Mean	SD
Hip positive	0.38	0.246
Hip negative	0.187	0.178
Hip net	0.193	0.235
Knee positive	0.432	0.334
Knee negative	0.104	0.117
Knee net	0.328	0.375
Ankle positive	1.99	0.613
Ankle negative	1.324	0.525
Ankle net	0.666	0.542
MTP positive	0.294	0.242
MTP negative	0.652	0.42
MTP net	-0.358	0.377